Research Article

A Paleo-Lake and wetland paleoecology associated with human use of the distal Old River Bed Delta at the Pleistocene-Holocene transition in the Bonneville Basin, Utah, USA

Manuel R. Palacios-Fest[a]* (iD), Daron Duke[b], D. Craig Young[c], Jason D. Kirk[d] and Charles G. Oviatt[e]

[a]Terra Nostra Earth Sciences Research, LLC; P.O. Box 37195, Tucson, Arizona 85740-7195, USA; [b]Far Western Anthropological Research Group, Inc.; 1180 Center Point Drive, Suite 100 Henderson, NV 89074, USA; [c]Far Western Anthropological Research Group, Inc.; 3656 Research Way, Suite 32. Carson City, NV 89706; [d]Department of Geosciences, University of Arizona, Tucson, AZ 85721, USA and [e]Department of Geology, Thompson Hall, Kansas State University, Manhattan, KS 66506, USA

Abstract

Mollusk and ostracode assemblages from the distal Old River Bed delta (ORBD) contribute to our understanding of the Lake Bonneville basin Pleistocene-Holocene transition (PHT) wetland and human presence on the ORBD (ca. 13,000–7500 cal yr BP). Located on U.S. Air Force-managed lands of the Great Salt Lake Desert (GSLD) in western Utah, USA, the area provided 30 samples from 12 localities. The biological assemblages and the potential water sources using $^{87}Sr/^{86}Sr$ analyses showed wetland expansion and contraction across the PHT, including the Younger-Dryas Chronozone (YDC). The record reflects cold, freshwater conditions, which is uncharacteristic of the Great Salt Lake Desert, after recession of Lake Bonneville. *Lymnaea stagnalis jugularis*, *Cytherissa lacustris*, and possibly *Candona* sp. cf. *C. adunca*, an endemic and extinct species only reported from Lake Bonneville, suggest cold-water environments. Between 13,000–12,400 cal yr BP, a shallow lake formed, referred to as the Old River Bed delta lake, fed by Lake Gunnison, as shown by $^{87}Sr/^{86}Sr$ ratios of 0.71024–0.71063 in mollusk fossils collected at the ORBD, characteristic of the Sevier basin. These findings add paleoenvironmental context to the long-term use of the ORBD by humans in constantly changing wetland habitats between 13,000–9500 cal yr BP.

Keywords: Late Quaternary, Paleo-Lake, Wetland, Mollusks, Ostracodes, Paleoecology, Paleoindian, Pleistocene, Early Holocene, Old River Bed, Western Stemmed

(Received 1 February 2021; accepted 3 July 2021)

INTRODUCTION

Reconstruction of paleoenvironments at the Pleistocene-Holocene transition (PHT) in North America has been the focus of much research over the last 100 years, and the basin of pluvial Lake Bonneville has served as a critical laboratory in the Desert West (e.g., Gilbert, 1890; Eardley, 1938; Currey, 1990; Morrison, 1991; Oviatt et al., 1994, 1999, 2005; Madsen et al., 2015a; Oviatt and Shroder, 2016). Changes in the terrestrial and stratigraphic records deposited during the late Pleistocene regressive phase of pluvial Lake Bonneville provide information on regional climatic drivers. Locally, these changes influenced the wetland habitats that were key to early occupation of the Great Basin by humans, ca. 13,000–9500 cal yr BP (Willig et al., 1988; Beck and Jones, 1997, 2015; Graf and Schmitt, 2007; Grayson, 2011; Madsen et al., 2015b; Smith et al., 2020).

Around the time of the Bølling-Allerød warming, ca. 15,000 cal yr BP, Lake Bonneville receded from its sill-controlled still-stand marked by the Provo shoreline, having stabilized for some time at that level following the catastrophic sill failure at Red Rock Pass. After 15,000 cal yr BP, evaporation outpaced input

from runoff and precipitation and the closed-basin lake regressed rapidly. Lake Bonneville's levels dropped precipitously and reached low-stands similar to the average elevation of the modern Great Salt Lake by 13,000 cal yr BP (Godsey et al., 2011; Oviatt, 2015). While the climate-driven pluvial lake retreated, however, an overflow river—the Old River Bed river—emanating from remaining surface connection to the Sevier drainage, flowed onto the basin floor as an inland delta (Oviatt et al., 2003; Madsen et al., 2015a; Bradbury et al., 2020) in what is now the southern extent of the Great Salt Lake Desert (GSLD) (Figure 1). This delta, and its associated water bodies and distributary network, is referred to herein as the Old River Bed delta (ORBD). As shown in Figure 1, many of its primary arterial channels have been mapped by aerial imagery and ground truthing during the course of archaeological research (Duke, 2011; Madsen et al., 2015a), but there is evidence for a vast network of eroded channels covering ~2,000 km^2 extending north of Knolls Dunes almost to Interstate 80 and into the western part of the basin toward Wendover, Utah (Madsen et al., 2015a; Clark et al., 2016, 2020). The characterization as an inland delta is best demonstrated for the early Holocene, to which most of the channels have been dated and have been the focus of archaeological work (Duke, 2011; Madsen et al., 2015a), but, as described in this study, the ORBD may have emptied into a large water body in the southern GSLD during the terminal Pleistocene. The ORBD
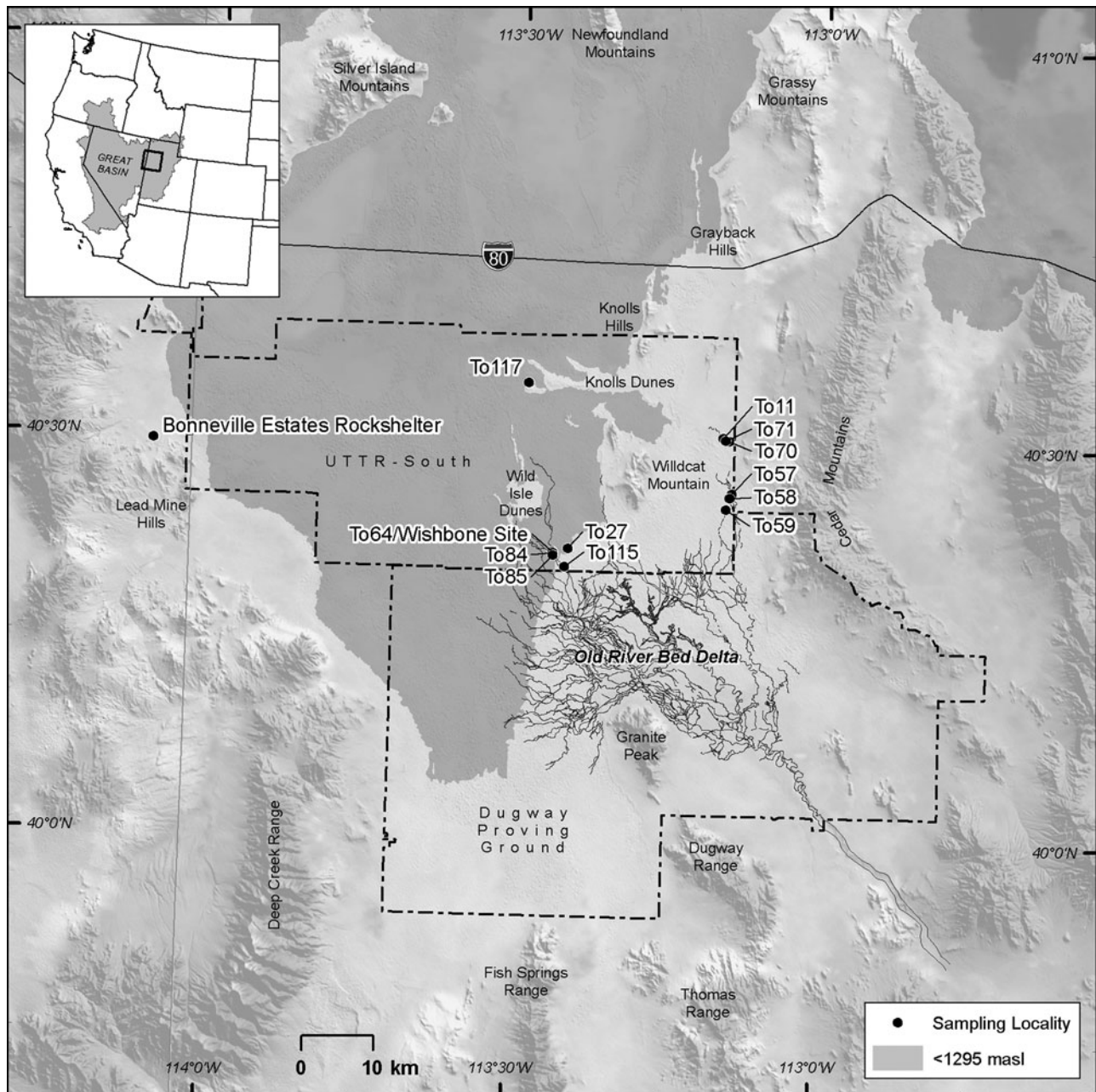
Figure 1. General location of the study area and sampling locations. Areas below the modern 1295-meter elevation contour within the Bonneville basin are shaded in gray. Black Channels of Madsen et al. (2015a) are shown in the map.

supported an extensive wetland complex and, for ca. 3500 years, sustained a primary wetland habitat and provided resources for human inhabitants (Arkush and Pitblado, 2000; Duke and Young, 2007; Schmitt et al., 2007; Duke, 2011, 2015; Madsen et al., 2015b; Madsen, 2016; Smith et al., 2020).

Question and purpose

While there has been significant study of Pleistocene transgressive and regressive cycles of pluvial Lake Bonneville (Oviatt and Shroder, 2016), our understanding of the dynamic response of ORBD landforms—distributary avulsions, inter-channel ponding, floodplain and levee stability, and occasional transgressive inundation—is evolving. The overlapping and occasionally cross-

cutting fluvial, paludal, and lacustrine facies present in the ORBD highlight a dynamic delta. What was the character of local environments preserved in the stratigraphic record of the ORBD, and how did they change through time? In this study, we focus on the paleoenvironmental record of mollusks, ostracodes, and the Sr-isotope signatures of groundwater from PHT sediments to clarify early post-Bonneville history in the northern part of the ORBD and relate it to human occupations that were among the earliest in the Great Basin.

ORBD non-marine mollusks and ostracodes are sensitive to environmental factors such as water temperature, salinity, and pH. In general, species and communities colonize, thrive, and retreat (or die) due to changes in water chemistry (Forester, 1991). Additional environmental variables, such as currents

(stream flow), turbidity, and bedload, influence population composition and maturity patterns (Rutherford, 2000; Dillon and Stewart, 2003). For example, pea clams (*Pisidium*) develop robust communities in well-oxygenated, lotic (flowing) waters, but do not colonize poorly oxygenated, lentic (slow-flowing or stagnant) waters where *Physella* flourishes. Similarly, terrestrial gastropods, such as *Oxyloma*, prefer riparian settings near water sources (Pilsbry, 1948). Based on our knowledge of modern communities, and inferences of past communities elsewhere, it is possible to infer past environmental conditions at localities where these organisms are found.

Here, we present results of collection and analyses of mollusks and ostracodes from 12 localities on the ORBD (Fig. 1). We open with a brief presentation of background on the regressive phase of pluvial Lake Bonneville, the formation of the ORBD, and human use. This is followed by the geography of the ORBD localities. Following a methods section, we provide detailed results on the biological composition of locality samples, supported by species identification and taphonomic patterns, and the $^{87}Sr/^{86}Sr$ ratio analysis of mollusk shells (*Stagnicola caperata*, *Valvata humeralis*, *Helisoma* (*Planorbella*) *trivolvis*, and *Gyraulus parvus*) at a few key localities. The results provide a generalized stratigraphy reflecting delta dynamics across the PHT. The stratigraphy includes a discussion of age control based on a suite of radiocarbon dates from natural organic-rich outcrops and excavated profiles. These serve as the basis for presentation and interpretation of six temporal biofacies evident in the stratigraphic and spatial record of the ORBD. We close with general discussion, conclusions, and recommendations for future study.

BACKGROUND

Gilbert (1890) was the first to recognize the ancient shorelines of what he would call Lake Bonneville and studied its dramatic transgressions and regressions based on field observations of its shorelines and sediments. Examination of early Holocene records in the Bonneville basin by Oviatt et al. (2003, 2015) identified evidence of freshwater on the basin floor at that time, most likely derived from groundwater discharge rather than from lake transgression. Oviatt (2014) described the Gilbert episode and reinterpreted the highest rise of Great Salt Lake (post-Lake Bonneville) at about the end of the Younger Dryas interval, ca. 11,500 cal yr BP.

Other efforts confirmed and refined these works (e.g., Currey 1990; Oviatt 2002, 2015; Benson et al., 2011; Godsey et al., 2011). In the Burmester core, Oviatt et al. (1999) found evidence of only four deep-lake cycles in Brunhes time (since 780 ka), the last of which is the Bonneville Lake cycle, which began ca. 30,000 cal yr BP. As Lake Bonneville retreated near the end of the Pleistocene, a lake in the main body (the Great Salt Lake basin) separated from the lake in the Sevier basin to the south (Oviatt et al., 2003). The Sevier basin lake is named Lake Gunnison (Oviatt, 1988). Lake Gunnison remained at its threshold as Lake Bonneville regressed, producing the river that flowed along the Old River Bed that debouched ~50 km to the north onto the basin floor in what is now referred to as the Great Salt Lake Desert (Madsen et al., 2015a). Overflow ceased at ca. 11,500 cal yr BP (Oviatt et al., 2003; Madsen et al., 2015a), but groundwater from the Sevier basin sustained the ORBD until ca. 9500 cal yr BP. Discharge from the Sevier basin continues today, although at less volume and to a lower water table. Sr-isotope signatures obtained in this and previous studies are consistent with this interpretation.

Human use

The first people to leave clear physical evidence of their presence entered the eastern Great Basin at approximately the beginning of the Younger Dryas chronozone (YDC). This evidence comes in the form of Western Stemmed Tradition (Smith et al., 2020) projectile points, stone tools, and radiocarbon-dated remains, usually hearths, found in the dry caves and rockshelters overlooking the Bonneville basin floor. Bonneville Estates Rockshelter, located in the Lead Mine Hills near Blue Lake ~60 km northwest of the area described in this paper (Fig. 1), contains an extensive record of Western Stemmed points and a series of hearths demonstrating human occupation beginning at least by ca. 12,900–12,700 cal yr BP (Goebel, 2007; Graf, 2007; Goebel and Keene, 2014; Goebel et al., 2021). Smith Creek Cave, located in the Snake Range overlooking the Snake Valley arm of the basin (~150 km southwest of the area described in this paper), contains similar evidence and timing (Bryan, 1979; Goebel and Keene, 2014). At both sites, a large, lanceolate projectile point type (known as Haskett) represents the first diagnostic Western Stemmed evidence (Duke, 2015). Goebel and Keene (2014) associate a hearth dating to $10,540 \pm 40$ ^{14}C BP (ca. 12,660–12,490 cal yr BP) with Haskett at Bonneville Estates Rockshelter. At Smith Creek Cave, several stem fragments are consistent with Haskett technology (Bryan, 1979) and are strongly associated with radiocarbon ages on four hearths and a piece of cordage considered by Goebel and Keene (2014) to represent the strongest evidence for the site's early occupation, ca. 12,600–12,100 cal yr BP. The location of these sites suggests that the extensive wetland resource base of the Bonneville basin—inclusive of the ORBD, but also including those fed by Deep Creek, Fish Springs, and other minor discharge distributaries—served as a key draw for the earliest substantial occupations by people in the region.

Sites such as these are not often preserved on the basin floor, but the horizontally distributed record of stone tools associated with the shifting hydrology of the ORBD through time provides some measure of human occupation (Duke, 2011; Madsen et al., 2015b). Hundreds of sites throughout the ORBD and alongside paleochannel landforms dating between ca. 12,300–9500 cal yr BP represent this association (Madsen et al., 2015a). One known exception, the Wishbone site (42TO6384; herein referred as To64), provides the first buried and stratigraphically intact evidence of people on the ORBD at ca. 12,300 cal yr BP (Duke et al., 2018a; Smith et al., 2020), as will be discussed in the current study. As in the early strata at Bonneville Estates Rockshelter and Smith Creek Cave, this site is directly associated with Haskett projectile points.

Projectile points are the most distinctive artifacts for tracking human use. They exhibit stylistically diagnostic modifications through time and are widespread at the ground surface of the ORBD (Duke, 2011; Beck and Jones, 2015). The points fall into two broad categories: the above-mentioned Western Stemmed Tradition and the split-/indented-base Pinto type. These occur in a relative early-to-late sequence, respectively, that has been observed elsewhere in the Great Basin, especially the Mojave Desert (see discussions by Haynes, 2004; Sutton et al., 2007). Together, they are associated with a cohesive lithic technological tradition strongly associated with regional wetland use (Duke, 2011; Grayson, 2011; Madsen et al., 2015b; Smith et al., 2020). Western Stemmed points represent a group of related styles with variably shaped stems. While their specific chronology is unclear, they are broadly time sensitive on the ORBD, with

those styles that are larger being older (e.g., Haskett, Cougar Mountain), and those that are smaller being younger (e.g., Silver Lake, Bonneville, Stubby) (Duke, 2011; Rosencrance, 2019; Smith et al., 2020). The larger styles, Haskett at least, are also largely associated with late Pleistocene, and the YDC specifically. Pinto represents a significant stylistic departure in the early Holocene at ca. 10,000 cal yr BP (Haynes, 2004; Janetski et al., 2012). This style exhibits an indented to split stem base, but no substantial change in point size from the smaller size that immediately precedes Western Stemmed styles. Of primary importance to the current study, the record of these point styles shows that people's intensity of use of the ORBD wetlands across the Pleistocene-Holocene transition increased as their long-range mobility decreased (Duke, 2011), likely by some combination of changing climatic conditions (Madsen et al., 2015a), the extinction of certain megafauna (Duke, 2015), and the disappearance of alternative basin wetland habitats to the ORBD (Duke, 2011; Duke and King, 2014).

Study area and sampling localities

The ORBD is in the southern GSLD in western Utah (Fig. 1). This study is an outgrowth of archaeological work conducted for the U.S. military, which emphasized an extensive record of early human presence in the desert west (Arkush and Pitblado, 2000; Duke and Young, 2007; Schmitt et al., 2007; Duke, 2011, 2015; Madsen et al., 2015b). The portion of interest here lies within the southern part of the Air Force's Utah Test and Training Range, where our research stems from cultural resources compliance inventories and limited archaeological excavations (Byerly et al., 2018; Duke et al., 2018a, 2018b). The geographic boundaries of the basin include the Cedar Mountains to the east, the Deep Creek Range to the southwest, and Granite Peak to the south, but the ORBD extends north into the central basin near the isolated geologic features of Wildcat Mountain and the Knolls hills (Clark et al., 2020).

The distal reaches of the delta of the ORBD include inverted gravel channels (Black channels of Madsen et al., 2015a) and a subtle, low-relief topography of weakly inverted sand channels, distributary meanders, meander and oxbow ponds and embayments, deflated mud flats, and occasional capping dunes. Delta features extend as far north as Interstate 80, extending over 60 kilometers from proximal segments preserved along the foot of Granite Peak.

To investigate spatial and temporal variability across the delta (and subject to limitations of access restriction), we focused on four areas of the delta (Fig. 1). The medial area between the inverted gravel channels and the Wild Isle Dunes (Localities To27, To64, To84, To85) is where archaeological test excavations revealed a thin (<1.5 m), but informative, stratigraphic section of the ORBD. Dateable, organic-rich black mats provide temporal markers interspersed in the delta facies with microfauna assemblages. The east delta localities comprise two clusters in distal delta channels and flats below the Cedar Mountains (Localities To57, To58, To59 on the generally open playa; Localities To11, To70, and To71 in the sandsheets and dunes further north). At these localities, black mats are exposed at the modern surface (or within a centimeter or two of the surface) where thin channel sands and silty muds preserve the organic wetland remnants. A single locality (To117) along the windward margin of the Knolls hills highlights the rare remnants of distal delta channels near the northernmost reaches of the distributary system. These distal delta channels are shown in Clark et al.'s (2016, 2020) DPG and BSF maps, respectively, and in Figure 1.

Materials and methods

The stratigraphy of the ORBD deposits is revealed where erosion from hydroaeolian planation (Currey, 1990, p. 193–194) exposed delta landform remnants in low-relief adjacent to channel forms and deflation basins. We also exposed detailed stratigraphic profiles in conjunction with geoarchaeological studies; these included archaeological units, geomorphological shovel probes, limited backhoe trenching, radiocarbon dating, and a preliminary core extraction. Such investigations have proven useful for defining broad temporal associations with the shifting hydrology of the distributary network for the otherwise undatable archaeological sites on the ground surface (Duke, 2011; Madsen et al., 2015b).

The presence of organic-rich black mat sediments has been crucial to reconstructing ORBD distributary chronology. Black mats are sedimentary strata altered by the accretion, inclusion, or penetration of organic material that draw our attention to profile sections and, in present-day arid environments such as the ORBD, highlight the likelihood that a profile may preserve a trove of information about environmental conditions unmatched in the modern setting (Quade et al., 1998, p. 129; Harris-Parks, 2016, p. 94). Although attempts have been made to characterize the black mats in time, space, and constituents (Harris-Parks, 2016), the label of "black mat" is applied to various dark, organic-rich strata or soil horizons that punctuate otherwise light-colored profiles (Haynes, 2008, p. 6520). Pigati et al. (2019, p. 52) refer to similar strata or horizons simply as "paleowetland deposits." Black mats have been especially informative in arid and semi-arid settings of the American Great Basin and Southwest where they mark the reactivation or formation of mesic habitats within the generally drying landscape of the Pleistocene-Holocene Transition (Quade et al., 1998; Haynes, 2008; Pigati et al., 2019). In the ORBD, black mats tend to mark sedimentary strata—often in multiple intercalated beds—that contain organic residues of former wetland habitats (decayed and carbonized plant and faunal remains), algal accretion in shallow water, and/or concentration of micronized charcoal reduced from wildfire flotsam and windrows along former shore zones. Due to the organic enrichment of these strata, although organic contributions may come from a variety of sources, they provide locally unique opportunities to define the spatial and temporal positions of the environments where they once formed.

To obtain the samples used in this investigation, we focused on collecting materials from geoarchaeological localities across the distal region of the ORBD, practically defined as the portion north of the UTTR-Dugway Proving Ground (DPG) military boundary (also see Madsen et al., 2015a) (Fig. 1). Geoarchaeological locality numbers were assigned to our sampling locations to make this distinction. We collected sediment samples for microfossils with cleaned trowels from sediment within stratigraphic layers. Target sample volume was ∼0.25–0.5 liters. At the laboratory, we analyzed the samples for mollusks and ostracodes. Mollusks were floated to separate the macro- and microfossils. Sample-size was ∼200 g, except for samples RBM-11 and RBM-14 that were 500 g each. We processed ∼100 g of sediments for the micropaleontological (ostracodes and micromollusks) analysis. The sediments were prepared using a set of three sieves (18 [1 mm], 140 [106 µm], and 230 [63 µm] US Standard) to retain the smallest valves and shells (Palacios-Fest, 2010). All samples were examined to identify fossil contents and biological assemblages. The biological composition included mollusks, ostracodes, and, rarely, gyrogonites

(Supplemental Tables 1, 2). All species were identified using reference collections, as well as the relevant literature on taxonomy by group (Wood, 1967; Delorme, 1970, 1971; Clarke, 1981; Dillon, 2000; Dillon and Stewart, 2003).

Mollusk shells were analyzed with a magnifying lens and measured with a digital caliper to determine the height, width, and aperture when appropriate. The samples were prepared using routine procedures described elsewhere (Palacios-Fest, 2010). A low-magnification microscope was used to identify the biological composition, diversity, abundance, maturity, and taphonomic features for micromollusks and ostracodes.

When possible, specimens were identified to the species level. Diversity, total and relative abundance, population density, and maturity (a ratio of the adult/juvenile shells) were recorded for reconstructing the paleoenvironmental history of the site. Other taphonomic parameters, such as fragmentation, abrasion, and encrustation, indicate the living and burial conditions of the shells. For example, a high degree of fragmentation and/or abrasion is interpreted as an indicator of transport (Adams et al., 2002), whereas increasing mineral overgrowth on the shells indicates excess salt concentration in the soils favoring the adherence of "exotic" minerals to the shells after burial (Adams et al., 2002). The maturity ratio allows us to differentiate a biocenosis (life assemblage) from a thanatocoenosis (death assemblage). That is, faunal assemblages consisting of a suite of adults and juvenile shells more frequently represent a local, living population (Whatley, 1983). By contrast, if juveniles or adults dominate the assemblage, it is possible to infer a thanatocoenosis that, in turn, may indicate the population is not local but either transported (if naturally) or selectively gathered (if by human activity).

We used 18 shell samples of four gastropod species (*Stagnicola caperata*, *Valvata humeralis*, *Helisoma* (*Planorbella*) *trivolvis*, and *Gyraulus parvus*) for strontium isotope ($^{87}Sr/^{86}Sr$) analysis. Each individual Sr analysis consisted of multiple shells with a combined total weight, depending on available material, of ~10–100 mg. The exceptions were samples To64-1-7-750, To27-1-1-15, and To84-1-6, which consisted of shell material weighing <1 mg. Shells were crushed and sonicated for 30 minutes in ultra-pure Milli-Q water (Millipore, 18.2 MΩ cm) and rinsed with Milli-Q until the solution was clear. After drying, the non-shell organic material was removed by sonicating the samples in 10% H_2O_2 (Fisher Chemical catalog number: H325) for 30 minutes. After rinsing the samples multiple times with Milli-Q water, the shells were then leached for five minutes in 5% glacial acetic acid (Sigma Aldrich catalog number: 338826) to remove non-shell carbonates.

The resulting shell material was then dissolved in 8M HNO_3 for separation of Sr. After dissolution, strontium was separated from samples using Sr resin (Sr-Spec Resin®, Eichrom, Lisle, Illinois, Part number SR-B100-A) and acid solutions made from twice-distilled acid. Separation procedures are modified from Horwitz et al. (1992). Strontium samples were loaded onto degassed Rhenium (Re) filaments using a TaF_5 activator (Charlier et al., 2006) to enhance ionization.

Strontium was analyzed using a VG Sector 54 multi-collector thermal ionization mass spectrometer in dynamic collection mode at the University of Arizona. The $^{87}Sr/^{86}Sr$ ratios were corrected for mass fractionation using $^{86}Sr/^{88}Sr = 0.1194$. NIST SRM 987 standards analyzed with the samples yielded a value of 0.7102406 ± 0.00001 (n = 2), and sample ratios were normalized to 0.710245 (Faure and Mensing, 2005). Total process blanks were an insignificant proportion of the total strontium separated from each sample.

Radiocarbon dating by Accelerator Mass Spectrometry (AMS) of material from black mat sediments and archaeological hearth charcoal provides our sample chronology. Where possible, samples were obtained from plant parts, if visible in the field, or from manual flotation in the laboratory; otherwise, bulk sediment was used. Samples were submitted to Beta Analytic (Beta) for pretreatment and analysis. Black mat plant remains are carbonized and resemble charred material. They may indeed be the product of low-temperature combustion, albeit not burned in the common sense, and therefore remain susceptible to instability in the base treatment. Beta's acid/alkali/acid pretreatment, typical for charred material, yielded adequate samples in each case and results that were consistent with stratigraphic expectations and the many prior dates collected on the ORBD (Madsen et al., 2015a). Bulk sediment was subjected to acid washes. In most cases, the black mats represent relatively short periods, on the order of a few hundred years or less, of waterbody (usually channel) activity and are thus not subject to averaging of long periods of time. They also have low potential for humate contamination given the sparse to barren nature of Holocene vegetation in the GSLD. More work could be done to clarify precision of the ages derived from our samples (see Pigati et al., 2019), but the results are appropriate to the temporal scale of comparison in the current study. Calibrated ages were generated using the IntCal20 curve (Reimer et al., 2020) calibration in the Calib 8.2 program (Stuiver et al., 2021).

Most of our sampling localities coincide with archaeological sites, although the latter vary from being directly or approximately associated to completely unassociated with the radiocarbon dates (see Table 1). Only one site is directly represented by charcoal from a human-made hearth and another by a charcoal lens that appears to represent another hearth. The Wishbone site (42TO6384) is definitive, with a fully excavated central hearth containing willow wood charcoal and a surrounding assemblage of food refuse (mostly waterfowl) and stone tools (Duke et al., 2018a). Site 42TO5136, the Hello site, is located ~200 m from Wishbone and is another Haskett-associated site found on the ground surface and eroding from a modern dissection in an ORBD landform (Duke et al., 2018b). Limited subsurface testing encountered a charcoal lens containing burned grass/sedge stems, willow wood, and waterfowl bone. The other sites have only indirect temporal associations (e.g., Pleistocene vs. Holocene age) with the radiocarbon or mollusk samples via proximity with dated ORBD landforms and strata. These estimations (Table 1) are based on assemblage information, especially time-diagnostic projectile points as discussed above, and horizontal spatial relationships with dated channel sets (Hirschi, 2006; Duke, 2011; Madsen et al., 2015a).

RESULTS

Stratigraphic sequence, temporal controls, and lithofacies

We define six major stratigraphic units (Fig. 2A, B). The distal delta channel landforms evident in whole or part at the study localities are related in one way or another to each of these units. The presence or absence of some strata depends on location within the study area.

Stratum I, which consists of blocky to marl-like clay and clayey silt indicative of deep water, sits atop Lake Bonneville marl. We do not know the timing of the transition to the Stratum 1 clay, but we estimate the age of regression of Lake Bonneville to elevations similar to that of the Wishbone site by 13,000 cal yr B.P., or as much as several hundred years earlier; greater precision is not

Table 1. Radiocarbon age estimates. *Calibrated ages rounded to decade. §Age Relationship represents an assemblage-based and distributary-associated age determination as Pleistocene (PL) or early Holocene (EH), followed by the site's direct or estimated relation to the calibrated median probability age of the dated sample (also see Materials and Methods).

| Beta Lab Number	Arch. Site/Age Relationship	Geo-locality, Sample No.	Sample Description	Stratum	Latitude	Longitude	Conventional ^{14}C age	δ^{13}C (‰)	Calibrated Median Probability Age*	Calibrated Age Range (95%)*§
355941	42TO0681/EH, approximate	To70, Sample RBM-01	Organic sediment	IV	40.50805	−113.15175	8050 ± 40	−22.6	8910	9090–8730
355942	42TO0681/EH, approximate	To70, Sample RBM-02	Organic sediment	IV	40.50877	−113.15228	7570 ± 40	−20.1	8380	8450–8220
355944	42TO5720/EH, unknown	To11, Sample RBM-04	Organic sediment	IV	40.51136	−113.16105	7380 ± 40	−23.8	8200	8330–8040
391201	42TO5755/EH, unknown	To71, Sample JO4 (Sample 2)	Carbonized plant remains	IV	40.50870	−113.15800	8720 ± 30	−13.8	9660	9890–9550
391202	42TO5720/EH, unknown	To72, Sample JO5 (RBM-03)	Carbonized plant remains	IV	40.51147	−113.16695	6660 ± 30	−11.5	7530	8580–7430
391204	42TO5734 & 42TO777/ EH, approximate	To57, Sample JO6 (RBM-06)	Carbonized plant remains – *Scirpus* seeds	IV	40.44179	−113.14599	8820 ± 30	−26.5	9850	10,120–9700
357212	42TO0774/EH, unknown	To59, Sample RBM-05	Organic sediment	IV	40.42167	−113.15523	7980 ± 40	−24.3	8850	9000–8650
357214	42TO5734 & 42TO777/ EH, approximate	To57, Sample RBM-07	Organic sediment	IV	40.44175	−113.14575	8560 ± 50	−24.7	9530	9660–9470
357215	42TO5734 & 42TO777/ EH, approximate	To57, Sample RBM-08	Organic sediment	IV	40.44005	−113.14631	8890 ± 40	−24.8	10,030	10,190–9800
n/a	42TO6384 (Wishbone)/ PL, direct	Three ages combined (see text)	Hearth charcoal	IV	40.36411	−113.43901	10,390 ± 20	-	12,270	12,470–12,060
471985	42TO5136 (Hello)	Locality To84-1, SP1, To84-1, Sample 2	Charcoal (possible hearth) – Grass/sedge stem	IV	40.36238	−113.43808	10,360 ± 40	−12.8	12,230	12,470–12,000
479061	42TO5135/PL-EH, post-dates >~400 cal yrs	To85-8, Sample 2	Organic sediment	II	40.35957	−113.43749	10,710 ± 30	−26.8	12,720	12,740–12,690
479063	42TO5136 (Hello)/PL, post-dates ~400 yrs	To84-1, Sample 5	Organic sediment	II	40.36236	−113.43802	10,670 ± 30	−27.2	12,700	12,730–12,620
479064	Non-site/none	To27-1, Sample 6	Organic sediment	II	40.36809	−113.41346	10,820 ± 30	−26.4	12,750	12,820–12,730
479065	42TO6384 (Wishbone)/ PL, post-dates ~400 yrs	To64-1, 2E/3N NE Quad, SP 1, Sample 8	Organic sediment	II	40.36411	−113.43901	10,690 ± 30	−27	12,710	12,740–12,670
479066	42TO6384 (Wishbone)/ PL, post-dates ~400 yrs	To64-1, 2E/3N NE Quad, SP 1, Sample 8	Organic sediment	II	40.36411	−113.43901	10,750 ± 30	−27.2	12,730	12,750–12,710
479067	42TO6384 (Wishbone)/ PL, post-dates ~400 yrs	To64-1, 2E/3N NE Quad, SP 1, Sample 8	Organic sediment	II	40.36411	−113.43901	10,790 ± 30	−27.3	12,740	12,760–12,720
479070	42TO6959/PL, post-dates ~400 yrs	To115-1, Sample 2	Organic sediment	II	40.34657	−113.41838	10,810 ± 30	−26.2	12,750	12,810–12,720
479071	42TO5135/PL-EH, post-dates >~300 cal yrs	To85-8, Sample 5	Carbonized plant remains/charcoal	II	40.35957	−113.43749	10,580 ± 40	−23.5	12,630	12,700–12,490
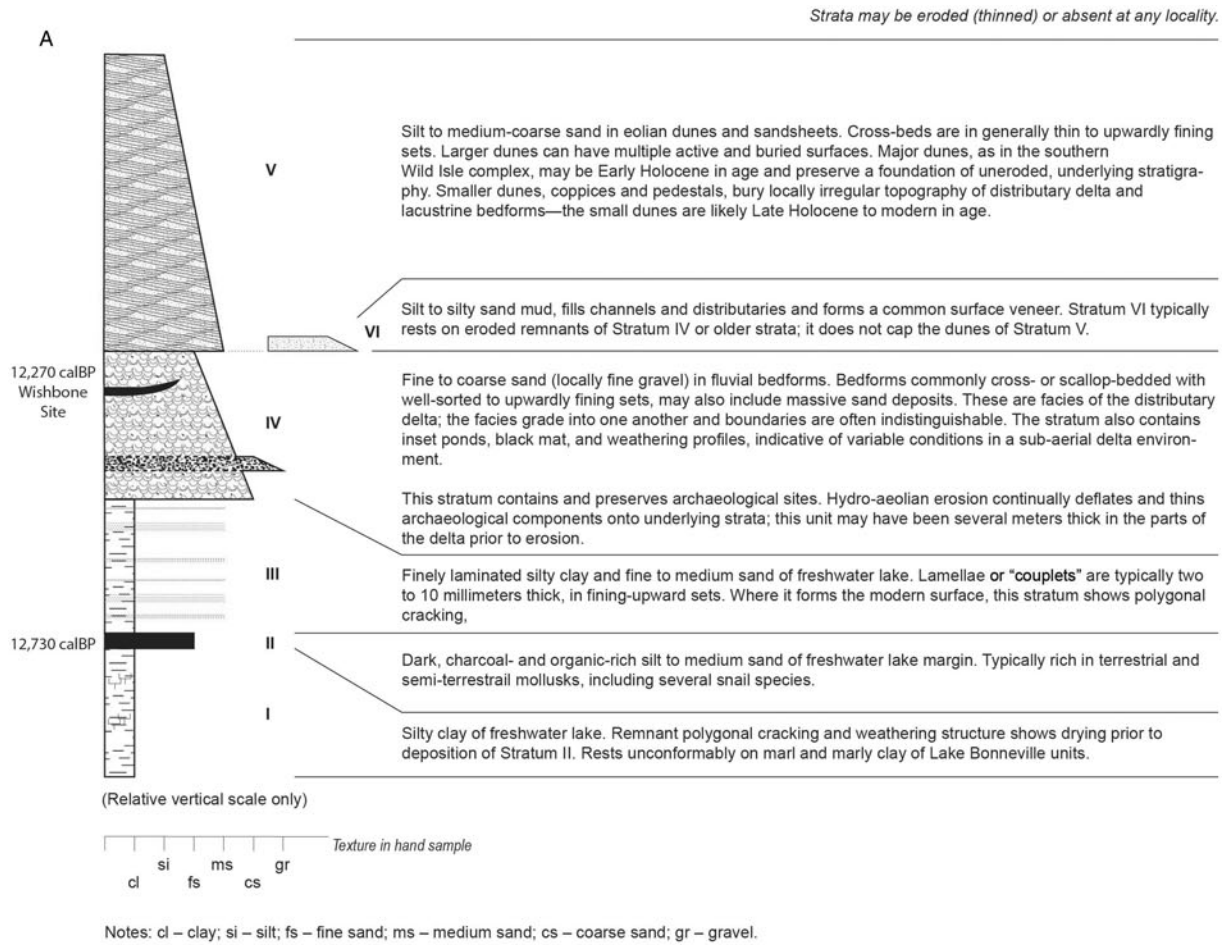
Figure 2. (A) Generalized stratigraphy; **(B)** Stratigraphic section at Locality To85-8, showing clear and abrupt contact between the sedimentary units. Stratum I is massive silty clay of freshwater lake; Stratum II is organic- and charcoal-rich silt to medium sand (black mat) of freshwater margin; Stratum III is finely laminated silty clay and fine to medium sand of freshwater lake; Stratum IV at modern surface is fine to coarse sand (locally fine gravel) of prograding delta; this deltaic stratum also contains inset ponds, black mat, and weathering profiles—facies common to the inland delta.

possible at this time (Godsey et al., 2011; Oviatt, 2015). Polygonal cracking at the Stratum I/II interface suggests an undetermined period of desiccation within the study area prior to a resurgence of lacustrine conditions that are represented by Stratum II.

Stratum II is a distinct organic- and charcoal-rich black mat that contains abundant terrestrial and semi-terrestrial mollusks. This prominent stratum is well dated, with multiple assays of carbonized wood fragments and organic sediment, and is found across a large area of the study area. Seven samples of Stratum II sediment provide a median probability calibrated age of 12,730 cal yr BP and a two-sigma range of 12,760–12,680 cal yr BP. The composition of Stratum II is similar to the YDC black mat elsewhere in North America, such as at Murray Springs, Arizona (Haynes and Huckell, 2007), Tule Springs (Haynes, 1967; Springer et al., 2015), and other sites around the world illustrated in Wolbach et al. (2018). Understanding that carbonized wood is mostly material that decayed in situ, and that charcoal is the result of burning, the visual physical appearance suggests widespread sorting of microscopic charcoal in water. We have no data to suggest the source of wildfires, or whether they might be naturally or culturally generated (but see Cushing et al., 1986; Rick et al., 2012; Lightfoot et al., 2013). However, during microscope work and fossil picking, the senior author recognized certain cubic forms of very small charcoal-like fragments. By contrast, in his personal experience, carbonized wood has a sapropelic appearance (amorphous).

Laminated clays alternating with clay-sand couplets form Stratum III. The prominent lobate Black channels of the proximal delta, now topographically inverted due to Holocene erosion, probably formed in the debouchment of the Old River Bed river into the shallow lake where Stratum III was forming. Stratum III, as with Stratum II, is distinct to our central basin sampling locations.

Stratum IV consists of sandy mud that contains localized black mats, finely laminated sands, and massive sand deposits. The vast bulk of what is known and dated of the ORBD represents Stratum IV deposits in the early Holocene to ca. 9500 cal yr BP, with decline thereafter. Our sample localities throughout the study area represent evidence of the stratum's persistence.

Erosion during middle to late Holocene time has differentially scoured landforms of the remnant delta. Erosion processes include hydroaeolian planation (Currey, 1990), which involves cyclic wetting and drying and deflation of fine-grained (silt- and clay-size) particles. Entrainment of fine-grained particles by raindrop impacts and sheetwash are likely to have been involved in the erosion. Coarser-grained particles (sand) are blown relatively short distances and end up in eolian dunes on the mudflat surfaces and at basin margins (Stratum IV). Strata V and VI represent dunes and the muddy veneer of the mudflats, respectively, and are the deposits of sediment that was eroded from the mudflat surface not far from the deposition sites. Strata V and VI unconformably overlie the eroded wetland strata in some places. Dunes of Stratum V often preserve the underlying geological and archaeological deposits, preserving pedestaled remnants of the delta (or other inverted landforms) that stand in low relief above the surrounding scoured landscape. In a few places, a relatively well-preserved archaeological record is locally evident at the stratigraphic boundary between Stratum III and Stratum IV.

Biological composition and biofacies

The ORBD samples contain a rich and diverse paleontological mollusk and ostracode assemblage (Table 2), which are

sometimes associated with calcareous algae. Supplemental Tables 1 and 2 summarize the ecological requirements of the mollusks and ostracodes, respectively, identified in this study. Figures 3 and 4 show the population density and relative abundance. Species associations with PHT radiocarbon age estimates (Table 1) show change through time in the local environment. Seventeen species of extremely rare to very abundant (1–756) gastropods and pelecypods were identified; whose adulthood ratios indicate a predominantly adult population, although juveniles are common. Twenty-three very rare to extremely abundant (5–3448) ostracode species were recovered. In both cases, we used the following abundance (numbers of individuals) bins: extremely abundant (>1000), very abundant (501–1000), abundant (101–500), moderately abundant (51–100), common (21–50), rare (6–20), and extremely rare (≤5). Suites of adults and juveniles characterize this group's stratigraphic distribution, whereas calcareous algae, only present in seven sites, are extremely rare to rare.

The taphonomic features indicate a broad range of fragmentation (2–60%), but limited abrasion (2–5%), and the shells are rarely oxidized (redox index). These patterns indicate mixed evidence of reworking and/or post-burial diagenetic effects (Whatley, 1983; Adams et al., 2002). A dysoxic ecosystem would commonly generate a light- to dark-gray coating of shells. By contrast, an oxidizing milieu would produce light- to dark-orange stains of the shell. Shells were mostly clear or white, rarely orange, implying well-oxygenated waters with no subaerial exposure, with one exception (Table 2).

With a change in lithology, we also identified a change in the biological composition. We have identified six biofacies across the PHT and potentially into the middle Holocene (ca. 13,000–7500 cal yr BP; Figs. 3, 4). Biofacies 1–4 correspond with the generalized stratigraphic units (I–IV) identified for reaches of the ORBD in the central southern GSLD, and the Wishbone site vicinity, while the later Biofacies (5 and 6) correspond to well-dated, near-surface sedimentary deposits of the delta nearer the east margin of the basin. Biofacies 5 and 6 are likewise found in deposits of the ORBD (i.e., Stratum IV), although they rest on older Lake Bonneville stratigraphy. The time periods for each biofacies represent the direct or constrained 95th percentile confidence ranges of associated radiocarbon ages (see Table 1), rounded to the nearest 100 years.

Biofacies 1 (ca. >12,900 cal yr BP)

Biofacies 1 corresponds with the deposition of Stratum I (Table 1). Its timing likely predates the YDC onset based on our numerous dates from immediately after the onset from Stratum II. The presence of polygonal cracking at the Stratum I/II interface suggests that the lake lowered to below the study area prior to rising again to deposit Stratum II. We anticipate that deposition of Stratum I, and the Biofacies 1 environment in which it was deposited, represents a period of hundreds, not thousands, of years based on what we know of the regression of Lake Bonneville through the area prior to 12,900 cal yr BP (Godsey et al., 2011; Oviatt, 2015)—effectively the onset of the YDC—but we do not have specific timing for our samples. Polygonal cracking at the top of Stratum I suggests a short dry period prior to the deposition of Stratum II.

Biologically, Biofacies 1 is dominated by the gastropods *Armiger crista*, *Planorbula campestris*, *Gyraulus parvus*, and *Helisoma (Planorbella) trivolvis*, and more rarely *Valvata humeralis* and *Fossaria parva*. The ostracode assemblage is composed of *Limnocythere itasca*, *Eucypris meadensis*, *Cyclocypris ampla*,

Table 2. Paleontological composition and taphonomic parameters. *Statistical count up to 300 specimens per sample. + = Mollusk float sample. § = Small sample collected for ostracodes only.

| Geo-locality, Sample No.	Stratum	Biofacies	Bulk Weight (g)	Fraction Weight (g)	Mollusks*	Adulthood Ratios	Ostracodes*	Adulthood Ratios	Fragmentation	Abrasion	Redox Index	Shell Color
+To70, RBM-01	IV	5	200.1	12.5	136	0.08	81	0.15	60	2	0	Clear
+To70, RBM-02	IV	5	200.	3.5	18	0.04	5	0.06	50	10	0	Clear
+To72, RBM-03	IV	6	175.2	1.6	1	-	0		10	5	0	White
To11, RBM-04	IV	5	201.8	7.2	69	0.04	96	0.30	30	2	0	Clear
+To59, RBM-05	IV	5	200.9	8.4	0	-	3448	0.03	2	2	0–2	Clear to Orange
+To57, RBM-06	IV	5	173.9	5	419	0.13	381	0.21	2	2	0	Clear
+To57, RBM-07	IV	5	176	10	383	0.09	358	0.22	2	2	0	Clear
+To57, RBM-08	IV	5	176.2	9.1	131	0.09	1998	0.21	2	2	0	Clear
+To71, Sample 2	IV	5	202.4	20	181	0.06	101	0.25	30	5	0	White
+To58, RBM-11	IV	4	500	14.6	380	0.19	510	0.29	50	2	0	White
+To117, RBM-14	IV	4	497.4	40.6	756	0.16	114	0.28	65	2	0	White
To84-1, Sample 6	I	1	94.2	2.9	50	0.08	332	0.21	30	2	0	Clear
To84-1, Sample 4	III	3	94.4	2.7	1	0.14	333	0.26	30	2	0	Clear
To84-1, Sample 1	IV	4	96.9	0.3	10	0.08	302	0.19	15	2	0	Clear
To84-1, Sample 3	IV	4	95.8	1.1	2	0.16	129	0.19	70	2	0	Clear
To85-8, Sample 7	I	1	86.1	2.9	117	0.08	301	0.29	30	2	0	Clear
To85-8, Sample 5	II	2	-	-	654	0.06	-	-	30	2	0	White
To85-8, Sample 4	II	2	85.1	7.6	300	0.15	326	0.17	30	2	0	Clear
To85-8, Sample 1	III	3	89.6	1.1	6	-	326	0.47	30	2	0	Clear
To64-1, Sample 10	I	1	91.8	12.5	134	0.27	340	0.17	30	2	0	Clear
To64-1, Sample 9	II	2	86.8	6.3	343	0.08	96	0.47	70	2	0	Clear
To64-1, Sample 7	III	3	92.0	6.7	11	0.16	352	0.17	30	2	0	Clear
To115-1, Sample 4	I	1	96.3	1.1	1	0.04	302	0.20	70	2	0	Clear
To115-1, Sample 1	II	2	97.5	3.8	19	0.11	330	0.20	30	2	0	Clear
To115-1, Sample 3	II	3	100.8	2.2	1	-	302	0.30	70	2	0	Clear
§To115-1, Sample 3	III	3	6.1	1.8	0	-	314	0.16	10	2	0	Clear
To27-1, Sample 4	I	1	99.3	5.9	300	0.02	334	0.23	30	2	0	Clear
To27-1, Sample 1	II	2	-	-	319	0.05	-	-	30	2	0	White
To27-1, Sample 3	II	2	97.2	4.7	319	0.04	347	0.08	30	2	0	Clear
To27-1, Sample 2	III	3	101.1	6.5	6	-	328	0.19	30	2	0	Clear
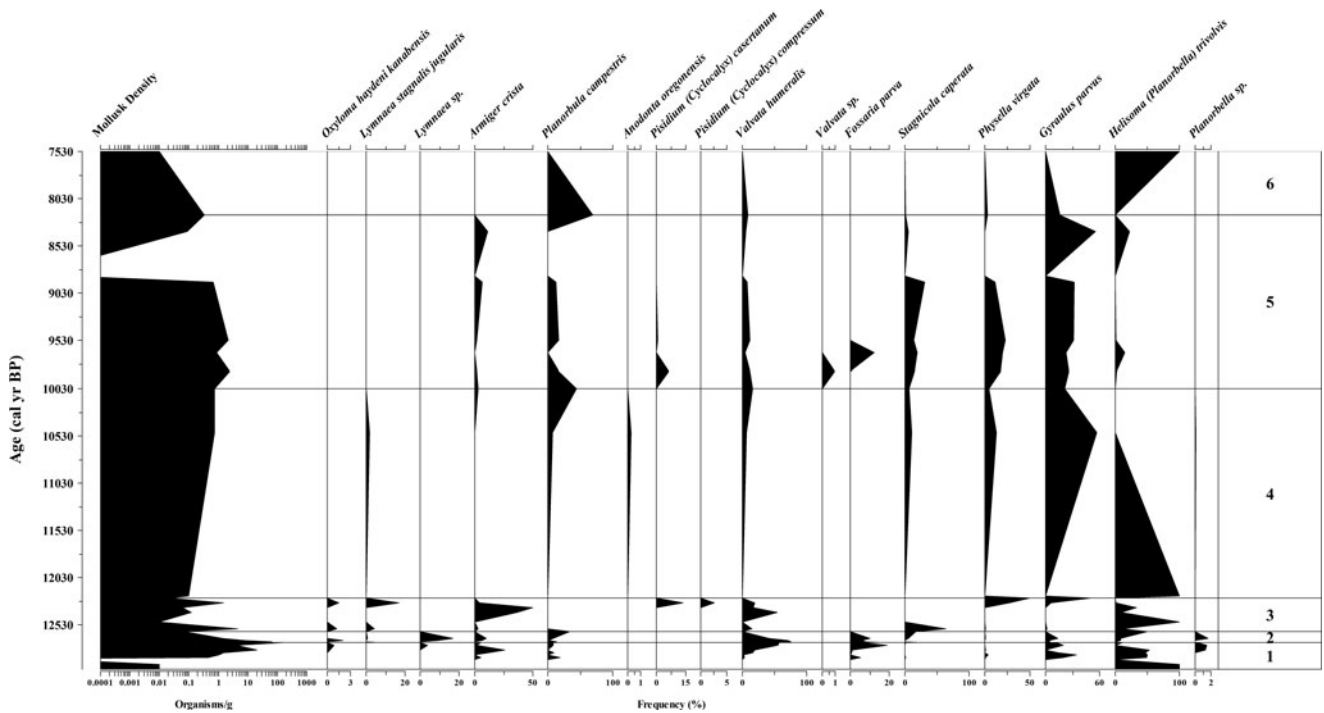
Figure 3. Mollusk biochronostratigraphy showing species relative abundance within the lithofacies and biofacies discussed in this investigation. Cold water indicators: *Planorbula campestris* and *Valvata humeralis* (see Supplemental Table 1).
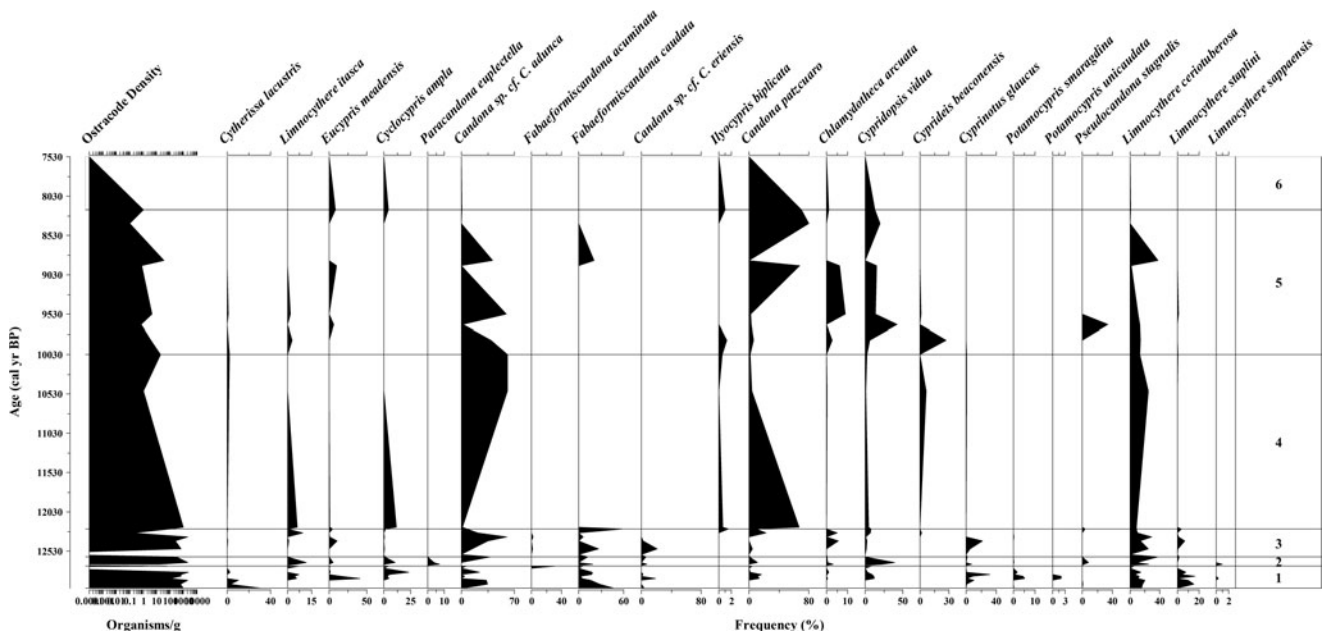

Figure 4. Ostracode biochronostratigraphy showing species relative abundance within the lithofacies and biofacies discussed in this investigation. Cold water indicators: *Cyclocypris ampla*, *Eucypris meadensis*, *Candona* sp. cf. *C. eriensis*, *Cytherissa lacustris*, *Limnocythere itasca* and *Fabaeformiscandona caudata* (see Supplemental Table 2).

Candona sp. cf. *C. adunca*, *Fabaeformiscandona caudata*, *Candona* sp. cf. *C. eriensis*, *Candona patzcuaro*, *Cypridopsis vidua*, *Cyprinotus glaucus*, *Potamocypris smaragdina*, *Potamocypris unicaudata*, *Limnocythere ceriotuberosa*, and intermittently *Cytherissa lacustris* and *Limnocythere sappaensis*. These species represent a generalized post Lake Bonneville subaquatic system that was still cold and possibly wet. Based on the

co-occurrence of *C. ampla* and *C. lacustris*, it is presumed that water temperature was <14°C.

Biofacies 2 (12,800–12,500 cal yr BP)
Biofacies 2 corresponds with Stratum II and represents a shallow (<∼2 m), lake-margin wetland. Its timing immediately post-dates the YDC onset based on a series of radiocarbon age estimates. The

total 95th percentile confidence range for the eight age estimates we have for Stratum II covers 300 years, but scrutiny of the probability areas of these suggests that this stratum was deposited in perhaps 100 years or less, ca. 12,700 cal yr BP.

The biological composition of Biofacies 2 consists of the mollusks *Oxyloma haydeni kanabensis, Lymnaea stagnalis jugularis, Lymnaea* sp., *V. humeralis, F. parva, G. parvus,* and *Planorbella* sp., with decreasing occurrences of *A. crista, P. campestris,* and *H.* (*P.*) *trivolvis.* The ostracode assemblage is dominated by *L. itasca, C. vidua, Pseudocandona stagnalis,* and *L. ceriotuberosa,* with the brief appearance of *Fabaeformiscandona acuminata, F. caudata, Candona* sp. cf. *C. eriensis, Chlamydotheca arcuata, Paracandona euplectella,* and *Cyprinotus glaucus.* The occurrence of *P. euplectella* and *P. stagnalis* advocate for a lakeside marsh environment, whereas the presence of *Ch. arcuata* suggests seasonal warm water input. These species represent the above-mentioned generalized environment that was still cold (~14°C) with warming episodes compared to before and after this unit.

Biofacies 3 (ca. 12,600–12,400 cal yr BP)

Biofacies 3 corresponds with the deposition of Stratum III. Stratum III indicates a deepening of the Stratum II lake to levels no longer supporting emergent lakeside marshes (these were presumably pushed to the south with the lake margin). We have no direct radiocarbon dating on Stratum III, and the 95th percentile confidence ranges for the underlying Stratum II and overlying Stratum IV end and begin at ca. 12,500 cal yr BP, respectively, leaving no intervening time. Here, we provide a working range of 12,600–12,400 cal yr BP for Biofacies 3 based on the relative probabilities associated with radiocarbon ages from Stratum II and Stratum IV, but we suspect a longer period. Biofacies 2/Stratum II is discussed above. Biofacies 4 is based on the dates for human-made hearths found within Stratum IV, ~50 cm above the Strata III/IV interface. Stratum IV represents varied sediments of the ORBD after the Stratum III-lake had receded and could have happened quickly, but Stratum III is ~30 cm thick at these sites, suggesting a lacustrine stand of some duration.

Biofacies 3 is dominated by the gastropods *A. crista* and *H.* (*P.*) *trivolvis,* with intermittent or minor occurrence of *P. campestris, V. humeralis, Stagnicola caperata, Physella virgata,* and *G. parvus.* The ostracodes associated with this biofacies include *Candona* sp. cf. *C. adunca, F. caudata,* and *L. ceriotuberosa,* with the rare appearance of *C. lacustris, E. meadensis, Candona* sp. cf. *C. eriensis, Ilyocypris biplicata, C. patzcuaro, Ch. arcuata, C. vidua, C. glaucus, P. stagnalis,* and *Limnocythere staplini.* These species represent fresher-water conditions than the previous Biofacies 2, with the intermittent occurrence of seasonal species such as *Ch. arcuata. Armiger crista, P. campestris,* and *V. humeralis,* along with *E. meadensis* and *Candona* sp. cf. *C. eriensis,* support a cold-water environment, once again <14°C. It represents the ORBD Lake.

Biofacies 4 (ca. 12,500–12,000 cal yr BP)

Biofacies 4 represents the environment at about the time of the Wishbone site occupation. As with Biofacies 5 and 6, it is found within Stratum IV deposits of the ORBD, but during the Pleistocene. Inclusive of both the human-made hearth at the Wishbone site and the charcoal lens/possible hearth at the nearby Hello site (Table 1), which are dated to effectively the same time, we apply an approximate age range of 500 years. Biofacies 4 is based on two samples from the latter site collected from Stratum IV immediately above (To84-1, Sample 1) and below

(To84-1, Sample 3) the charcoal lens. We thus assume that the age range is generally representative of Biofacies 4 and that Biofacies 4 is representative of the paleoenvironment at the times of the Wishbone and Hello site occupations.

The mollusk composition of Biofacies 4 contains *H.* (*P.*) *trivolvis, G. parvus, P. virgata,* and more rarely *S. caperata, V. humeralis, Anodonta oregonensis, L. stagnalis jugularis,* and *O. haydeni kanabensis. Candona patzcuaro, C. ampla, L. itasca,* and to a lesser concentration *Cyprideis beaconensis, I. biplicata, C. vidua,* and *L. ceriotuberosa* constitute the ostracode assemblage of Biofacies 4. Unexpectedly, *Candona* sp. cf. *C. adunca* is abundant throughout Biofacies 4. The unique presence of *A. oregonensis* indicates slow-flowing to stagnant wetland conditions, in sandy to silty substrates. These species represent a generalized environment with increasing temperature (>14°C, but ≤20°C; Supplemental Table 2). This is the ORB Delta cooler stage.

Biofacies 5 (10,200–8000 cal yr BP)

Biofacies 5 is again from the ORBD (Stratum IV), but represents a late early Holocene environment from ca. 10,200 cal yr BP until approximately the onset of the middle Holocene. This represents an 1,800-year gap from the end of the Biofacies 4 interval, but only because we did not sample the intervening time frame. We do not know at what time the transition between the two environments occurred, or if there might be other distinguishable biofacies.

Biofacies 5 is composed of the mollusks *P. virgata* and *G. parvus,* with a decreasing occurrence of *P. campestris, V. humeralis, S. caperata,* and *A. crista. Lymnaea stagnalis jugularis, O. haydeni kanabensis* and the pea clams *Pisidium* (*Cyclocalyx*) *casertanum* and *P.* (*C.*) *compressum* are restricted to the base of the record, whereas *H.* (*P.*) *trivolvis* is extremely rare throughout the biofacies. The ostracodes include *Candona* sp. cf. *C. adunca, L. ceriotuberosa, C. patzcuaro, Ch. arcuata, C. vidua,* and more rarely *F. acuminata, C. beaconensis, I. biplicata, L. staplini,* and *P. stagnalis,* which occur intermittently throughout. However, *E. meadensis* reappears towards the top of the record to prevail in Biofacies 6. The faunal assemblage advocates for warming conditions relative to Biofacies 4. Estimated water temperature would have ranged from 13–24°C or more as the area was desiccating.

Biofacies 6 (ca. 8600–7400 cal yr BP)

Biofacies 6 is within the middle Holocene and suggests persistent surface groundwater and limited remnant wetlands between ca. 8600–7400 cal yr BP based on the 95th percentile confidence range of a single date (Table 1). Uppermost Biofacies 6 only contains the mollusks *H.* (*P.*) *trivolvis.* No ostracodes were present in this interval. The sole occurrence of *H.* (*P.*) *trivolvis* indicates the ORBD was desiccating to a status similar to today where there is surface groundwater and wetland habitat in the GSLD.

The strontium isotope evidence

The measured [87]Sr/[86]Sr ratios are presented in Supplemental Table 3 and Figure 5. Samples To84-1-Sample 6, To64-1-Sample 7, and To27-1-Sample 1-15 are presented in Supplemental Table 3, but their data are not included in the resulting regressions or Figure 5 because the small amount of material and/or the low concentration of these samples precluded precise measurement of the [87]Sr/[86]Sr ratios and the resulting uncertainty is much larger than the normal and accepted precision levels.
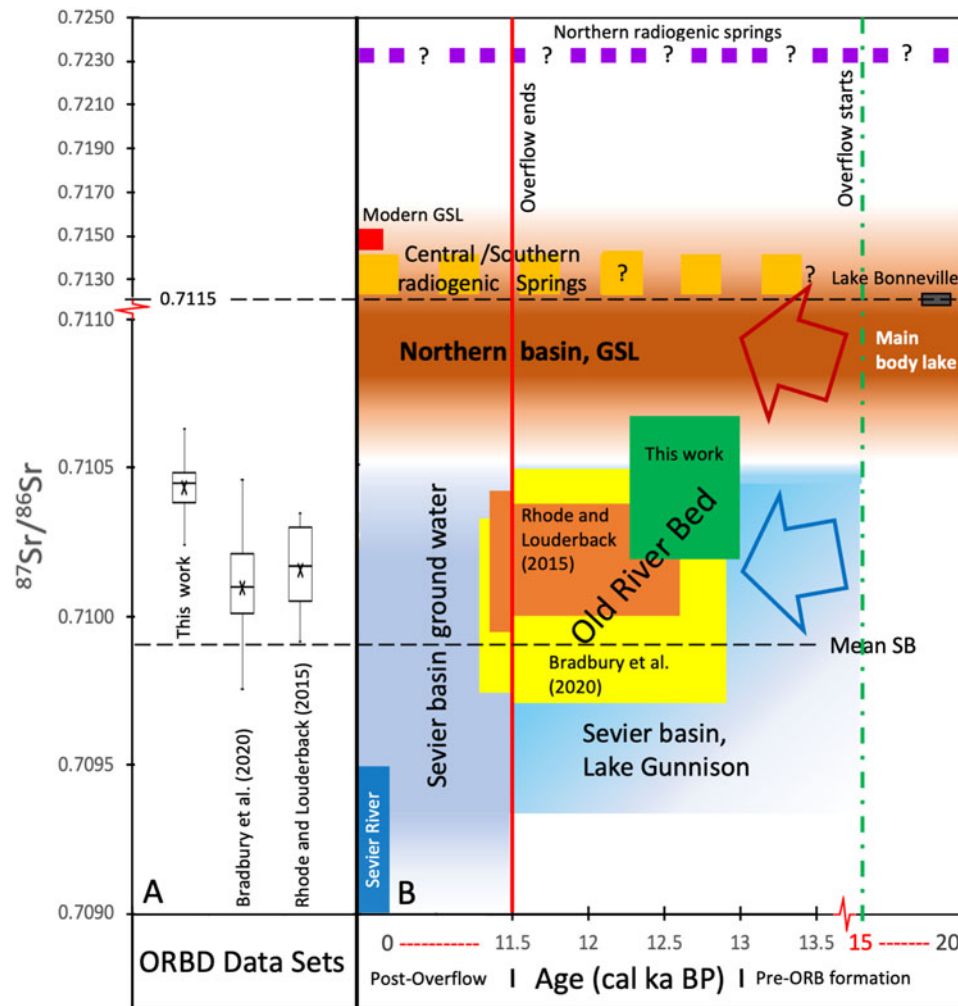
Figure 5. (A) Box plots of $^{87}Sr/^{86}Sr$ ratios of gastropods from Rhode and Louderback (2015), Bradbury et al. (2020), and this work. The mean values are specified with an X. **(B)** Schematic diagram comparing the ranges of $^{87}Sr/^{86}Sr$ ratios of various water sources through time and of gastropods from the Old River Bed Inland Delta. Age is in cal yr BP and centered around ages of likely Gunnison overflow (note scale change at 11,500 cal yr BP and 14,000 cal yr BP). The vertical scale has a scale change at 0.7110 to accommodate the much more radiogenic values of northern water sources. The vertical dashed green line at 15,000 cal yr BP marks the age of likely onset of overflow from Lake Gunnison via the ORBID into the northern basin (Godsey et al. 2011). The red vertical line marks cessation of overflow at ~11,500 cal yr BP (Oviatt, 1988). See text for discussion.

The gastropods in this study have $^{87}Sr/^{86}Sr$ ratios between 0.71025–0.71063, with a mean value of 0.71044. Stratigraphic correlations and superposition result in calibrated ages for the samples of between 12,250 to >12,750 cal yr BP. The $^{87}Sr/^{86}Sr$ ratios and calibrated ^{14}C ages of the two other published data sets of gastropods from the ORBD are also shown in Figure 5. The $^{87}Sr/^{86}Sr$ ratios of Rhode and Louderback (2015) range from 0.70991–0.71035 (mean of 0.71016), with ages between 9990–12,570 cal yr BP (rounded to nearest decade). The data of Bradbury et al. (2020; Rust channel sample excluded because the authors concluded direct influence of extant stream water) has a larger overall range in $^{87}Sr/^{86}Sr$ ratios and ages, with values between 0.70975–0.71046 (mean of 0.71010) and 9300–12,900 cal yr BP, respectively. Despite the larger overall range of $^{87}Sr/^{86}Sr$ ratios, the Bradbury et al. (2020) dataset has a very similar mean to the Rhode and Louderback (2015) dataset. In contrast, our dataset has an appreciably more radiogenic average $^{87}Sr/^{86}Sr$ ratio of 0.70144. The two published datasets also include samples from the period after Lake Bonneville had dropped below

the ORBD threshold (~1395 m), although no significant difference in the range of $^{87}Sr/^{86}Sr$ values is observed in these younger 9300–11,500 cal yr BP samples. The Bradbury et al. (2020) and Rhode and Louderback (2015) samples are from the proximal ORBD, 10–15 km to the southeast.

DISCUSSION

Lake Bonneville had regressed to below our study area sometime after 15,000 cal yr BP, and probably between 14,000–13,000 cal yr BP (Godsey et al., 2011; Oviatt, 2015). Our geomorphological data demonstrate that the basin nevertheless remained wet, with a large waterbody, which we call the Old River Bed lake (ORBDL), at ~1295 m asl; the ORBDL occupied a large area in the GSLD (Fig. 1). This lake is represented by Strata I and III. The ORBD channel system originated in this context, extending northward from where the ORB river emptied onto the flat basin floor in the area now occupied by Dugway Proving Ground. The lake margins shifted and the lake reshaped itself

through time causing the delta margins to shift—at times fluvial channels emptied into the lake, and at other times the delta formed a widespread inland distributary system that did not empty directly into the lake. By the early Holocene (Madsen et al., 2015a) the ORBD supported extensive wetlands. Our mollusk and ostracode data track well with this characterization, showing a shift from colder to warmer behind the changes that ultimately resulted in complete desiccation in the middle Holocene. These changes had implications for human populations, which were likely drawn to the rich and developing wetlands on the ORBD.

The biological composition of mollusks and ostracodes reached its highest diversity in samples from ORBDL Stratum I, reflecting cold conditions, lowered evaporation, and surface water input prior the onset of the YDC. Many species established a biocenosis. Figure 3 shows a diverse mollusk and abundant ostracode population. Ostracodes are also diverse and rich (Fig. 4). Locally, *L. sappaensis*, *C. glaucus*, *C. lacustris*, and *Candona* sp. cf. *C. adunca* are common. However, *Candona* sp. cf. *C. adunca* is not abundant in this interval. *Cytherissa lacustris* is erratic throughout the area, but most abundant in Locality To115. The occurrence of the Holarctic species *P. campestris* (snail) and the ostracodes *C. ampla* and *C. lacustris* indicates a shallow, cold-water environment with a salinity no higher than 300 mg/L total dissolved solids (TDS) (Curry et al., 2012). Based on the temperature tolerance listed in Supplemental Table 2 for ostracodes, we infer that water temperature during deposition of Biofacies 1 was <14°C (Bunbury and Galweski, 2009). The co-occurrence of *C. ampla* and *C. lacustris* during this interval is consistent with boreal conditions (Curry and Baker, 2000) and with higher dissolved oxygen concentrations (>3 mg/L) in an oligotrophic to mesotrophic setting (Belis et al., 2008). The ^{87}Sr/^{86}Sr ratios of Stratum I show some of the highest values recorded in this study, ranging from 0.71033–0.71048 (Supplemental Table 3). These values suggest that, at this time, Lake Gunnison (0.70912–0.71049 ^{87}Sr/^{86}Sr ratios) contributed freshwater to Stratum I.

There is currently no direct indication of people using the ORBD in Stratum I times, although we know they had begun occupying the region by at least 12,900 cal yr BP based on radiocarbon dates on hearth features at Bonneville Estates Rockshelter on the west margin of the basin (Graf, 2007; Goebel and Keene, 2014; Smith et al., 2020; Goebel et al., 2021). We surmise that the developing wetland habitat of the ORBD to the south (i.e., up the gradient and above the level of the ORBDL) was a key draw to the area for these people (also see Madsen et al., 2015b).

The dark, organic- and charcoal-rich sedimentary deposit of Stratum II hosts a diverse ostracode and mollusk assemblage consisting of a mixed population of adults and juveniles indicating an in situ assemblage (>1:5 adulthood ratios). The dominant ostracode species in Biofacies 2 (Stratum II) across the area are *F. acuminata*, *C. vidua*, *F. caudata*, *L. ceriotuberosa*, *L. itasca*, and *Candona* sp. cf. *C. adunca*, although their occurrence throughout the southern GSLD is uneven (Fig. 4). Gastropods *V. humeralis* (the most abundant across the area), *F. parva*, *S. caperata*, and *G. parvus*, *A. crista*, *H.* (*P.*) *trivolvis*, and *Oxyloma haydeni kanabensis* (juveniles) are present in this unit (Fig. 3).

The ostracodes from Stratum II include two species, *L. sappaensis*, and *P. euplectella*, not recorded elsewhere in the ORBD, although neither of them is abundant. In the case of *L. sappaensis*, the scarce shells might have been reworked. *Paracandona euplectella*, however, fits well with the hypothesis

that the black mat was deposited in a lakeside wetland or extended shallow pond. To the best of our knowledge, this is the first report of *P. euplectella* in the southern GSLD. The assemblage, however, is consistent with a spring-fed system or perennial lentic stream discharge into a peat bog or a vast, shallow wetland. The disappearance of *C. lacustris* and occurrence of *L. itasca* and *Cypridopsis vidua* may be associated with freshwater conditions from groundwater influx and/or additional freshwater sources (Pfaff et al., 2005) generating more mesotrophic conditions than during Biofacies 1. Based on the temperature range of the ostracode faunal assemblage, the site was still cold (<14°C), but the water was shallower and with greater groundwater influx (Supplemental Table 2). The ^{87}Sr/^{86}Sr ratios range between 0.71024–0.71063, still under the influence of Lake Gunnison.

As with Biofacies 1, there is no direct indication of human occupation of the ORBD at this time. Any location where Stratum II was identified in the current study would have been under water (Fig. 1). We do not know how far the waterbody in which Stratum II was deposited would have extended, but based on its location and elevation, the area would have been a shallow wetland with abundant emergent vegetation for 10 km or more in the northwest-southeast direction and unavailable to humans. Much as with Stratum I, people may have accessed peripheral areas in Stratum II times, but we do not have direct evidence for this.

The rich and diverse microinvertebrate fauna (ostracodes and mollusks) of Biofacies 3, representing the depositional environment of Stratum III, indicates that a shallow lake occupied the GSLD for, at least, 200 years and received alternating input of ground water and runoff during the time Biofacies 3 existed. The fossils in this unit show little abrasion, implying in situ deposition in a permanent water body. The slow flow of horizontal currents introduced the superposed layers of ostracode valves throughout the area. The abundance of *Candona* sp. cf. *C. adunca* and *L. ceriotuberosa* in the ostracode-only lens implies that the site became deeper, contrasting with the mollusk signature across the area. Shallow, weedy environments containing abundant root casts support this interpretation. The ostracode lens is consistent with a brief deepening episode during deposition of Stratum III in response to water-table fluctuations or wet-dry events that characterized a fluctuating climate during the YDC. These deposits' marly nature supports the hypothesis that this stratum is a facies deposited in the ORBDL.

The ostracode marl of Stratum IV (in which abundant carbonate grains were identified under the microscope) contains mollusk shells and ostracodes of Biofacies 4. Figures 3 and 4 show the transition from freshwater to saline water in an increasingly drier environment in the upper half of Stratum IV (Fig. 4). Increasingly drier conditions are inferred from the association of *C. vidua*, *C. patzcuaro*, and *L. ceriotuberosa* despite the dominance of *F. caudata*, which is consistent with Delorme's (1969, p. 1473) interpretation of the *Candona rawsoni* group (*C. patzcuaro* belongs to this group). The four species tolerate a wider range of environmental conditions, although *F. caudata*'s temperature range is more limited than that of the associated fauna. Temperature unlikely exceeded 20°C (Supplemental Table 2).

Humans visited the Biofacies 4 environment, as demonstrated at the Wishbone site (42TO6384; To64), which contains stone tools, waterfowl bones (food refuse), and two Haskett-style projectile points of the Western Stemmed technological tradition (Duke et al., 2018a; Smith et al., 2020). The central hearth at the site yielded three statistically consistent willow-wood charcoal

dates (10,370 ± 30, 10,370 ± 40, 10,430 ± 40 ^{14}C BP) with a combined radiocarbon age of 10,390 ± 20 ^{14}C BP (ca. 12,300 cal yr BP) (Table 1). The Wishbone site occupants took advantage of the newly formed wetland, occupying linear dry, streamside landforms that provided deep access to the ORBD marshes. The nearby Hello site was occupied at about the same time, based on the date from a charcoal lens that appears to be a hearth. The Biofacies 4 samples are from immediately above and below this lens, and thus generally represent the environment at the time of these occupations. The timing of Biofacies 4 is tied to the age of the site hearths, which could extend as late as ca. 12,000 cal yr BP, but continuous human occupation of the ORBD wetlands (and deposition of Stratum IV), as represented by Western Stemmed and Pinto points, is well established through the early Holocene (Duke, 2011; Madsen et al., 2015b).

A eurytopic faunal assemblage characterized Biofacies 5, beginning ca. 9500 cal yr BP. Ostracodes are abundant, but then decline abruptly after ca. 7900 cal yr BP. Five ostracode species dominate (*F. acuminata, L. ceriotuberosa, C. patzcuaro, C. vidua,* and *Ch. arcuata*), with rare appearances of *L. itasca* and *C. lacustris*. The latter is occasional but consistent throughout most of the unit. Mollusks are also the most diverse and abundant in this phase. The species associated with Biofacies 5 include *G. parvus, V. humeralis, P. virgata,* and *P. campestris*. Two species, *L. stagnalis jugularis* and *O. haydeni kanabensis*, occur only at the base of the record. At a time of gradually rising temperatures, it is inferred that Biofacies 5 indicates a period of dilute, cold-water input into the wetlands through groundwater discharge in the ORBD area that originated in the Sevier basin (Oviatt et al., 2003, 2015; Madsen et al., 2015a; Rhode and Louderback, 2015; Bradbury et al., 2020) (Figs. 3, 4). However, these biofacies likely reflect constant water temperature and water chemistry changes, as shown in Supplemental Table 2. The temperature range during Biofacies 5 was 13–24°C, the upper limit for *C. beaconensis*, and the lower limit for *Ch. arcuata*.

The temporal range for Biofacies 5 is significant in that it largely post-dates the bulk of early Holocene channels of the ORBD, which formed early in that time interval (ca. 11,700–10,200 cal yr BP), and represent its maximum active wetland size (Madsen et al., 2015a). This interval also represents the most intensive period of occupation by people (Duke, 2011; Madsen et al., 2015b). Madsen et al. (2015b, p. 239) reported 70 radiocarbon age estimates on black mat plant material or organic sediment from across the ORBD and found the majority to date to this period; only five, dating between ca. 9900–9100 cal yr BP, occur within the time of Biofacies 5. Thus, we have effectively bookended the period of intensive human use of the ORBD with the data herein and do not know when the transition from Biofacies 4 to 5 occurred. Madsen et al. (2015b, p. 49) described the period of our Biofacies 5 as marking "…the last pulses of wetland environments. As surface flow stopped reaching the Wild Isle and Wildcat reaches of the delta, wetland productivity would have become increasingly isolated, until replaced by a generally desiccated playa and dune landscape."

Our paleoenvironmental data support this interpretation, and the archaeological data do as well. People appear to have substantially diminished or even discontinued their use of the ORBD between ca. 9800–9500 cal yr BP, with the emergence of ground stone use for intensive seed processing at Danger Cave at the basin margin near Wendover, Utah, at about the same time (Rhode et al., 2006). Our Biofacies 5 samples come from the east distal delta, east of Wildcat Mountain, and are associated

with late-dating ORBD channels that were not previously recognized (Fig. 1). Duke (2011) argued that archaeological patterning changes through time alongside shifting distributary output in a west-to-east manner on the distal portion of the ORBD between Wild Isle Dunes and Wildcat Mountain. This spatial pattern is shown in a temporal framework by a shift from large projectile points, such as the Haskett style from Wishbone to smaller Western Stemmed styles and Pinto; the east delta region sites are dominated by Pinto over Western Stemmed.

Biofacies 6 is marked by the sharp disappearance by the middle Holocene of the cold-water indicators typical of Biofacies 5. The sole occurrence of *H.* (*P.*) *trivolvis* indicates a semi-arid environment that periodically flooded, which permitted arrival of this pulmonate snail. Biofacies 6 may be interpreted as a desiccation episode as the area evolved into the semi-arid region of today (mean low of 5°C; mean high of 19°C). The poor record prevents us from inferring the temperature range at this interval, but we estimate temperatures >20°C.

Although surface water representing the last vestiges of the ORBD was present for Biofacies 6, it was not likely associated with the bulk of the archaeological record in the east delta. This interval is well understood to be too late for Western Stemmed projectile points, and Pinto points do not appear to have persisted to this time either. The best spatial association between sites and dated channels in the area suggests most human activity dates to the early part of the Biofacies 5 period (ca. 10,200–9500 cal yr BP). The minor wetlands of Biofacies 6 may represent spot occurrences of surface groundwater along relict, otherwise desiccated, ORBD channels during short cool/wet periods versus a declining persistence of the ORBD per se. The presence of a few large, corner-notched points not otherwise found on the ORBD, but consistent with those seen in nearby caves and rockshelters in times consistent with Biofacies 6 (Hoskins, 2016; Hockett and Goebel, 2019), may be the representative archaeological signature for these final wetlands.

Regression of Lake Bonneville as a closed-basin lake was probably caused by global or hemispheric dry climatic conditions coincident with the Bølling-Allerød Interstadial (14,700–13,300 cal yr BP) (Godsey et al., 2011). The Bølling-Allerød Interstadial was followed by the YDC (Rasmussen et al., 2006; Steffensen et al., 2008; Cheng et al., 2020), which is of particular interest in the context of this paper. Cheng et al. (2020) gave the following bounding ages for the YDC: 12,870 ± 30 to 11,600–11,700. If these ages are rounded off to the nearest 100 yr, the duration of the YDC lasted from ca. 12,900–11,700 cal yr BP, or for 1200 yr.

Literature on the climate of the YDC in western North America is vast, but the following references are pertinent to interpretations of YDC paleoclimate in the Bonneville basin (e.g., Quade et al., 1998; Wigand and Rhode, 2002; Oviatt et al., 2005; Hall et al., 2012). It is possible that part of the apparent spatial variability in YDC climate that has been documented in western North America (Meltzer and Holliday, 2010) is a function of temporal variability in climate during the ca. 1200 years of the YDC (perhaps climate was cool and dry early in the YDC, then became cool and wet later in the YDC?). Different authors working in different places and with different proxies have concluded that YDC climates were wet and cool, dry and cool, warm and wet, or other possibilities (Meltzer and Holliday, 2010). Precision and accuracy of dating control, gradual accumulation of more and better evidence, and the evolution of thoughts and interpretations, may also be factors in the lack of agreement

among studies. Although it is possible to legitimately arrive at different interpretations of YDC climate, it seems likely that in the Bonneville basin climate was relatively cool and dry compared to times immediately before and after the YDC (Oviatt, 2014; Rhode, 2016); in this paper we adopt this interpretation.

Two ostracode species are particularly relevant in this investigation because of their limited occurrence and apparent association with cold- and/or deep-water environments: *Cytherissa lacustris* and *Candona* sp. cf. *C. adunca*. *Cytherissa lacustris*, described initially from deep lakes (Delorme, 1970; Delorme and Zoltai, 1984), is currently known to live in shallow, spring-fed wetlands of the Arctic Circle (Bunbury and Gajewski, 2009; Krzymińska and Namiotko, 2011), which resemble the ORBD environments. It is a geographically widespread species distributed from shallow to deep waters (as deep as 200 m in Lake Constance, Switzerland; Meisch, 2000), but common at 20–30 m depth (e.g., Mondsee, Austria; Danielopol, 1990). A cold stenothermic form, *C. lacustris* thrives better in oligo-mesotrophic lakes, but it is also common in shallow systems. Anthropogenic eutrophication affects it severely (Wilkinson et al., 2005). Forester (1987) reported *C. lacustris* from shallow, cold groundwater-fed wetlands in Lake Bonneville. Oviatt (2017) argued that *C. lacustris*, an important marker in Lake Bonneville marl, thrives in cold water with low total dissolved solids (TDS) (Delorme, 1969). *Cytherissa lacustris* is not common in this basin, but appears in response to pulses of cold, fresh groundwater into the lake. We cannot discard the possibility that the specimens of *C. lacustris* in our samples have been reworked because the carapace is robust and easily transported with no damage. However, the occurrence of adults and juveniles advocates for a local population.

Candona sp. cf. *C. adunca*, the endemic and extinct ostracode species of Lake Bonneville, was found by Lister (1975) in cores taken by A.J. Eardley from the southeast margin of Great Salt Lake (the Saltair and Section 28 cores), but he did not provide stratigraphic details. The species appears to be restricted to the late transgressive phase of Lake Bonneville and persisted into the early regressive phase when Lake Bonneville was freshest (Oviatt, 2017). The specimens identified here as *Candona* sp. cf. *C. adunca* correspond well with Lister's (1975, p. 10) original description and illustrations of the species.

Our specimens are identical to Oviatt's (2017, fig. 4) illustration of the species. Lister (1975) highlighted the pronounced posteroventral projection of the outer margin. Like Lister's species, our specimens lack the pronounced posterodorsal hump characterizing *Fabaeformiscandona caudata*. In terms of size, *Candona* sp. cf. *C. adunca* in this study is larger than *F. caudata* and in the same size range of those of Lister (1975) and Oviatt (2017). The possibility exists that our specimens could be another form of *Fabaeformiscandona* (such as *F. acuminata*), but a higher posterodorsal hump distinguishes our specimens of *F. acuminata*. It is a puzzle to precisely interpret *Candona* sp. cf. *C. adunca* in the ORBD wetland deposits; we think it is likely that the specimens identified in this study as *Candona* sp. cf. *C. adunca* are indeed the species. A possibility that we think is less likely, but which we haven't been able to fully evaluate, is that *Candona* sp. cf. *C. adunca*, and perhaps other ostracodes, were reworked in low-energy conditions from older Lake Bonneville deposits.

As far as we are able to determine, *Candona* sp. cf. *C. adunca* lived in cold-water environments. What seems more relevant, though, is that it is associated with other cold-water indicators, such as the ostracode *L. itasca* and the gastropod *P. campestris*.

Their co-occurrence with more fragile forms such as *L. itasca* suggests all these species co-existed. To the best of our knowledge, *Candona* sp. cf. *C. adunca* has not been found in non-Bonneville marl deposits in the southern GSLD. This is the first formal report of *Candona* sp. cf. *C. adunca* in the area that appears to be supported by the $^{87}Sr/^{86}Sr$ isotopes identified in deposits of the ORBD.

The $^{87}Sr/^{86}Sr$ ratios of Rhode and Louderback (2015) range from 0.70991–0.71035 (mean of 0.71016), with ages between 9,990–12,570 cal yr BP (rounded to nearest decade). Irrespective of the differences in the datasets, all samples except To84-1-6, To27-1-3-10, and To27-1-1-14 (all from Stratum II) are within the range of values of Lake Gunnison (0.70930–0.71049; mean of 0.70989; Hart et al., 2004). Rhode and Louderback (2015, p. 25, Table 2.1) used the fact that their $^{87}Sr/^{86}Sr$ values are within the range of Lake Gunnison values to conclude that there was "continued overflow from Lake Gunnison via the ORBD or leakage of groundwater from the Sevier basin through alluvium." Bradbury et al. (2020) cited the geomorphological studies of Oviatt et al. (2003) that support high energy flow through the older channels of the ORBD to posit that their older samples had a Lake Gunnison water source via overflow as well. They also concluded that their samples younger than the likely age of the cessation of overflow at ca. 11,500 cal yr BP (Oviatt, 1988) were sourced from groundwater from the Sevier basin, which is thought to likely have a comparable Sr isotopic range as the former Gunnison waters (Madsen et al., 2015a; Rhode and Louderback, 2015).

Because their data are bound by the Gunnison values, Rhode and Louderback (2015) and Bradbury et al. (2020) ruled out both Sr influx from more radiogenic northern water sources (Gilbert-episode lake; Oviatt, 2014) and discharge from mountain and piedmont aquifers recharged during Lake Bonneville times (Oviatt et al., 2015; Schmitt and Lupo, 2018), respectively. Their Sr data as well as ours, however, do not rule out either of these as contributors to the waters of the ORBD (as well as not ruling out radiogenic spring contributions; see Hart et al., 2004; Bradbury et al., 2020). For example, mixing between non-radiogenic Sr reservoirs, such as an earlier version of the Sevier River and one or multiple radiogenic reservoirs present at the time, could produce all of the ORBD $^{87}Sr/^{86}Sr$ values. Radiogenic spring water contribution to ORBD sediments is discussed in Bradbury et al. (2020), but insufficient evidence exists of a direct radiogenic contribution by spring water to the ORBD during the period of interest, or of how the inputs may have varied across the area.

A significant or sole role for Lake Gunnison for our samples is also possible. The three data points of ours that outlie the composition of Lake Gunnison are at most only 0.00014 greater. By contrast, $^{87}Sr/^{86}Sr$ ratios of samples from Lake Gunnison (Hart et al., 2004) have a range of 0.0012, which is almost an order of magnitude larger variation. It is likely that Lake Gunnison (and later groundwaters from the Sevier basin) would have an even larger range of $^{87}Sr/^{86}Sr$ than the seven samples measured by Hart et al. (2004). This is supported by a Sr study on carbonate dust (Carling et al., 2020) that shows dust from the dry bed of Sevier Lake with $^{87}Sr/^{86}Sr$ values between ~0.7097–0.7108, but with a similar mean (0.71008), as in-place carbonates (0.70989; Hart et al., 2004).

There are a number of non-unique paths between Sr reservoirs at the time of the ORBD deposition that either solely or in conjunction with other reservoirs could have produced the results.

However, because of geomorphologic, stratigraphic, hydrologic, and the other lines of evidence presented by the various, previously cited authors, our preferred interpretation also agrees with that of Bradbury et al. (2020) and Rhode and Louderback (2015)—namely that the $^{87}Sr/^{86}Sr$ values of ORBD gastropods result from the influx of Lake Gunnison waters prior to the cessation of overflow. The samples of the other datasets that are younger than the cessation of overflow have similar results, and therefore Lake Gunnison-sourced ground water is plausible. However, data from all of the ORBD samples do not preclude contribution by or mixing between less- and more-radiogenic water sources. In other words, the whole of the ORBD Sr data is inconclusive on the source of Sr in these samples, but are not contradictory to models of early overflow from Lake Gunnison and later Sevier basin groundwater.

Three of the six biofacies identified in this investigation suggest intervals of shallow lake and wetland formation in the southern GSLD during the YDC that we refer to as the ORBDL. Strata I and III contain ostracodes and mollusks that indicate a lacustrine environment, with ostracode species typically found in cold freshwater habitats. A facies similar to that of Strata I and III has not been found previously in the Bonneville basin, and its presence indicates that, despite the likely dry climate, the basin floor was very wet at the time Strata I and III were being deposited. One possibility for the interpretation of Strata I and III is that an extensive water body or lake existed in the GSLD at those times. The maximum elevation of occurrences of Stratum III near the Wishbone site is close to 1295 m, and if that elevation were to be taken as the shoreline of the lake and traced around the GSLD, the line would connect with Great Salt Lake (Fig. 1). Such a lake would have been very large, but shoreline landforms or offshore sediments of this age have not been recognized. Another possible interpretation of Strata I and III is that the sediments were deposited in lakes that were confined by landforms, such as natural levees, associated with the ORBD wetland system. Qualifying landforms are not apparent now in the GSLD, but considering the extensive Holocene-aged deflation in this area (Oviatt et al., 2003; field observations as part of this study), it is possible that confining landforms could have been present while the ORBDL was present, but are now erased from the landscape. For this paper, we prefer the interpretation that Strata I and III were deposited in a large, but short-lived lake because that interpretation is consistent with the available observations. More information is needed to be certain.

By contrast with Pigati et al. (2014), Springer et al. (2015), and Forester et al. (2016), who associated hypogean ostracodes with groundwater discharge, we did not find them in sediments deposited in samples from Strata I and III, even though we sieved our sediments using a 63 μm (230 US Standard) sieve to separate the sand fraction from the finer sediments. Based on the faunal association identified in ORBDL, it is likely that seasonal flooding introduced detrital sediments to the area during the rainy season(s). The system apparently remained flooded during episodes of groundwater input, as suggested by the alternating grayish/whitish laminae characterizing Stratum III, but lake-level declined briefly during deposition of Stratum II.

The ORBD shows some similarity to the paleowetlands of the Okavango Delta in South Africa. For example, Stratum IV was deposited in paleowetlands, the deposits of which now are flanked by topographically inverted paleochannels; the wetlands were seasonally flooded, as were those described by McCarthy and Ellery (1998). However, Strata I and III contain a lacustrine fauna that

thrived in a permanent lake for, at least, 200 years. While the Okavango Delta created a mosaic of wetland habitats in different successional stages due to the constant change in primary channels, the paleowetlands of ORBD show no significant variation in faunal composition within each stratum (Figs. 3, 4).

The PHT across North America marks a change in human land-use, shifting from a wide-ranging, hunting-based subsistence economy to a more local and plant-oriented focus. There is no direct evidence of human occupation of the study area in Biofacies 1–3, but restricted anthropogenic use of peripheral areas towards the south, or proximal ORBD (where the elevation was higher), is possible. The human occupants of the Wishbone site in the GSLD arrived at ca. 12,300 cal yr BP between deposition of Biofacies 3 and the beginning of deposition of Biofacies 4. At the Wishbone site, a waterfowl-associated cooking feature and Haskett projectile points demonstrate that these hunting-and-gathering people moved and camped along the intervening dry landforms between wetland channels early in the Stratum IV depositional episode. Deposition continued as the ORBD endured through the early Holocene until the wetlands gradually desiccated and disappeared (Duke, 2011; Madsen et al., 2015b).

CONCLUSIONS

Sediments in the ORBD contain a rich and diverse fauna that shows the composition and changing environmental conditions in the southern GSLD following recession of Lake Bonneville. We found evidence of a large body of cold, freshwater in the GSLD beginning prior to the YDC and persisting into the YDC —a time during which the climate was relatively dry but also conducive to low evaporation rates. Our hypothesis is that Strata I–III represent facies of what we call the ORBDL, which fluctuated in depth for several hundred years and contained a lacustrine fauna. Humans took advantage of a vast and verdant freshwater marshland associated with river flow and groundwater discharge in the southern GSLD forming the ORBDL and expanded into the vast ORBD distributary network by the early Holocene. The mollusk data track well with the multiple lines of paleoenvironmental evidence showing a transition to warmer conditions by the early Holocene, leading to the ORBD's ultimate desiccation by, or intermittently within, the middle Holocene.

The archaeological record of the ORBD provides a trajectory of change through time that corresponds well with the paleoenvironmental data. The earliest observable occupations of the Bonneville basin begin ca. 13,000 years ago, and developing marshlands associated with the ORBDL and feeding distributaries were likely the key draw. In our study area, the ORBDL receded and was replaced by meandering channels of the ORBD by the mid-YCD. Warmer conditions in Biofacies 4 are apparent at this time, and people were able to access this area on dry streamside landforms, as evinced at the Wishbone site, ca. 12,300 cal yr BP. Haskett projectile points indicative of this time are common to the Wishbone site vicinity, but are uncommon across the greater ORBD (Duke 2011, 2015; Beck and Jones, 2015), suggesting that the human population in the terminal Pleistocene was small. Later, Western Stemmed styles and a transition to Pinto attest to extensive human emphasis on the ORBD during the early Holocene. We know this from the chronology of ORBD channels provided by the various archaeological and paleoenvironmental work of others (Duke, 2011; Madsen et al., 2015b), but we do not have data representing this time in our study. Our Biofacies 5 demonstrates

furthering warming conditions by ca. 10,200 cal yr BP during a period of the late early Holocene that largely post-dates the era of intensive use. We took a bookend approach to examining the paleoenvironment in the current study, and future work should sample black mats dating between ca. 12,000–10,200 to clarify the environment during this interval, especially to determine the transition between biofacies 4 and 5 (e.g., whether it was gradual or precipitous), or if there are other distinguishable biofacies; there are many channels of known age to choose from to address these issues. By Biofacies 6 times, representing the early part of the middle Holocene, the ORBD was largely desiccated with a minor area of persistent or intermittent groundwater in its eastern region near the base of the Cedar Mountains. Whatever water resources remained were apparently insufficient to draw frequent visits from the people of the Bonneville basin.

REFERENCES

Adams, K.R., Smith, S.J., Palacios-Fest, M.R., 2002. *Pollen and micro-invertebrates from modern earthen canals and other fluvial environments along the Middle Gila River, Central Arizona: implications for archaeological interpretation*. Gila River Indian Community, Anthropological Research Papers No. 1, Sacaton, Arizona, 76 pp.

Arkush, B.S., Pitblado, B.L., 2000. Paleoarchaic surface assemblages in the Great Salt Lake Desert, northwestern Utah. *Journal of California and Great Basin Anthropology* 22, 12–42.

Beck, C., Jones, G.T., 1997. The terminal Pleistocene–early Holocene archaeology of the Great Basin. *Journal of World Prehistory* 11, 161–236.

Beck, C., Jones, G.T., 2015. Lithic analysis. In: Madsen, D.B., Schmitt, D.N., Page, D. (Eds.), *The Paleoarchaic Occupation of the Old River Bed Delta*. The University of Utah Press, Salt Lake City, Utah, pp. 97–208.

Belis, C.A., Lami, A., Guilizzoni, P., Ariztegui, D., Geiger, W., 2008. The late Pleistocene ostracod record of the crater lake sediments from Lago di Albano (Central Italy): changes in trophic status, water level and climate. *Journal of Paleolimnology* 21, 151–169.

Benson L.V., Lund, S.P., Smoot, J.P., Rhode, D.E., Spencer, R.J., Verosub, K.L., Louderback, L.A., Johnson, C.A., Rye, R.O., Negrini, R.M., 2011. The rise and fall of Lake Bonneville between 45 and 10.5 ka. *Quaternary International* 235, 57–69.

Bradbury, C.D., Jewell, P.W., Fernandez, D.P., Lerback, J.C., DeGraffenried, J.V., Petersen, E.U., 2020. Water provenance at the Old River Bed inland delta and ground water flow from the Sevier basin of Central Utah during the Pleistocene-Holocene transition. *Quaternary Research* 99, 114–127. https://doi.org/10.1017/qua.2020.66.

Bryan, A.L., 1979. Smith Creek Cave. In: Touhy, D.L., Randall, D.R. (Eds.), *The Archaeology of Smith Creek Canyon, Eastern Nevada*. Nevada State Museum Anthropological Papers 17, Carson City, pp. 162–253.

Bunbury, J., Gajewski, K., 2009. Biogeography of freshwater ostracodes in the Canadian Arctic Archipelago. *Arctic* 62, 324–332.

Byerly, R., Duke, D., Young, D.C., Rice, S.K., 2018. *Cultural Resources Inventory of 6,575 Acres of the West Delta of the Old River Bed, Utah Test and Training Range, Tooele County, Utah*. Contract Report, Far Western Anthropological Research Group, Inc., Henderson, Nevada.

Carling, G.T., Fernandez, D.P., Rey, K.A., Hale, C.A., Goodman, M.M., Nelson, S.T., 2020. Using strontium isotopes to trace dust from a drying Great Salt Lake to adjacent urban areas and mountain snowpack. *Environmental Research Letters* 15, 114035. https://doi.org/10.1088/1748-9326/abbfc4.

Charlier, B.L., Ginibre, C., Morgan, D., Nowell, G.M., Pearson, D.G., Davidson, J.P., Ottley, C.J., 2006. Methods for the microsampling and high-precision analysis of strontium and rubidium isotopes at single crystal scale for petrological and geochronological applications. *Chemical Geology* 232, 114–133.

Cheng, H., Zhang, H., Spötl, C., Baker, J., Sinha, A., Li, H., Bartolomé, M., et al., 2020. Timing and structure of the Younger Dryas event and its underlying climate dynamics. *Proceedings of the National Academy of Sciences* 117, 23408–23417.

Clark, D.L., Oviatt, C.G., Page, D., 2016, *Geologic map of Dugway Proving Ground and adjacent areas, Tooele County, Utah, scale 1:75,000*. Utah Geological Survey Map 274DM, GIS data, 31 p. https://ugspub.nr.utah.gov/publications/maps/m-274/m-274txt.pdf.

Clark, D.L., Oviatt, C.G., Hardwick, C.L, Page, D., 2020. Interim geologic map of the Bonneville Salt Flats and east part of the Wendover 30′ x 60′ quadrangles, Tooele County, Utah, Year 3, scale 1:62,500. *Utah Geological Survey Open-File Report* 731, 30 pp. https://doi.org/10.34191/OFR-731.

Clarke, A.H., 1981. *The Freshwater Mollusks of Canada*. National Museums of Canada, Ottawa.

Currey, D.R., 1990. Quaternary paleolakes in the evolution of semidesert basins, with special emphasis on Lake Bonneville and the Great Basin, USA. *Palaeogeography, Palaeoclimatology, Palaeoecology* 76, 189–214.

Curry, B.B., Baker, R.G., 2000. Paleohydrology, vegetation, and climate since the late Illinois Episode (∼130 ka) in south-central Illinois. *Palaeogeography, Palaeoclimatology, Palaeoecology* 155, 59–81.

Curry, B.B., Delorme, L.D., Smith, A.J., Palmer, D.E., Stiff, B.J., 2012. The biogeography, and physicochemical characteristics of aquatic habitats of freshwater ostracodes in Canada and the United States. In: Horne, D., Holmes, J.A., Rodriguez-Lazaro, J., Viehberg, F.A. (Eds.), Ostracoda as Proxies for Quaternary Climate Change. *Developments in Quaternary Science* 17, 85–115. https://doi.org/10.1016/B978-0-444-53636-5.00006-8.

Cushing, J., Wenner, A.M., Noble, E., Daily, M., 1986. A groundwater hypothesis for the origin of "fire areas" on the Northern Channel Islands, California. *Quaternary Research* 26, 207–217.

Danielopol, D.L., 1990. On the interest of the "Cytherissa" project and the present state of researches. In: Danielopol, D.L., Carbonel, P., Colin, J.P. (Eds.), *Cytherissa the Drosophila of Paleolimnology*. Bulletin de l'Institut de Geologie du Bassin d'Aquitaine 47, 15–26.

Delorme, L.D., 1969. Ostracodes as Quaternary paleoecological indicators. *Canadian Journal of Earth Sciences* 6, 1471–1476.

Delorme, L.D., 1970. Freshwater ostracodes of Canada. Part III. Family Candonidae. *Canadian Journal of Zoology* 48, 1099–1127.

Delorme, L.D., 1971. Freshwater ostracodes of Canada. Part V. Families Limnocytheridae, Loxoconchidae. *Canadian Journal of Zoology* 49, 43–64.

Delorme, L.D., Zoltai, S.C., 1984 Distribution of Arctic ostracode fauna in space and time. *Quaternary Research* 21, 65–73.

Dillon, R.T., Jr., 2000. *The Ecology of Freshwater Molluscs*. Cambridge University Press, New York.

Dillon, R.T., Jr., Stewart, T.W., 2003. *The Freshwater Gastropods of South Carolina*. Electronic document: http://www.cofc.edu/~FWGNA/FWGSC.

Duke, D., 2011. *If the Desert Blooms: A Technological Perspective on Paleoindian Ecology in the Great Basin from the Old River Bed, Utah* [Ph.D. Dissertation]. Department of Anthropology, University of Nevada, Reno, Nevada.

Duke, D., 2015. Haskett spear weaponry and protein-residue evidence of proboscidean hunting in the Great Salt Lake Desert, Utah. *PaleoAmerica* 1, 109–112.

Duke, D., King, J., 2014. A GIS model for predicting wetland habitat in the Great Basin at the Pleistocene-Holocene transition and implications for Paleoindian archaeology. *Journal of Archaeological Science* 49, p. 276–291.

Duke, D., Young, D.C., 2007. Episodic permanence in Paleoarchaic basin selection and settlement. In: Graf K., Schmitt, D. (Eds.), *Paleoarchaic or Paleoindian? Great Basin Human Ecology at the Pleistocene-Holocene Transition*. The University of Utah Press, Salt Lake City, Utah, pp. 123–138.

Duke, D., Rice, S.K., Young, D.C., Byerly, R., 2018a. *The Playas Archaeological Inventory: 6,194 Acres on the Utah Test and Training Range Including Portions of the West Distal Delta of the Old River Bed*

and Test Excavations at the Wishbone Site (42TO6384), Tooele County, Utah. Far Western Anthropological Research Group, Inc., Henderson, Nevada.

Duke, D.D., Young, C., Rice, S.K., 2018b. Cultural Resources Inventory of the High-Speed Mover Test Area, a 4,548-acre Portion of the West Delta of the Old River Bed, Utah Test and Training Range, Tooele County, Utah. Far Western Anthropological Research Group, Inc., Henderson, Nevada. [Copies available from State No. U12FF0788m]

Eardley, A. J., 1938. Sediments of the Great Salt Lake, Utah. American Association Petroleum Geologists Bulletin 22, 1305–1411.

Faure, G., Mensing, T.M., 2005. Principles and applications. John Wiley & Sons, Inc., Hoboken, New Jersey, 879 pp.

Forester, R.M., 1987. Late Quaternary paleoclimate records from lacustrine ostracodes. In: Ruddiman, W.F., Wright, H.E. Jr. (Eds.), North America and Adjacent Oceans During the Last Deglaciation. Geology of North America K-3. Geological Society of America, Boulder, Colorado, pp. 261–276.

Forester, R.M., 1991. Ostracode assemblages from springs in the western United States: implications for paleohydrology. Memoirs of the Entomological Society of Canada 155, 181–201.

Forester, R.M., Carter, C., Quade, J., Smith, A.J., 2016. Aquifer and surface-water ostracodes in the Quaternary paleowetland deposits of southern Nevada, USA. Hydrobiologia DOI 10.1007/s10750-016-2966-5

Gilbert, G. K., 1890. Lake Bonneville. U.S. Geological Survey Monograph 1, 275 pp.

Godsey, H.S., Oviatt, C.G., Miller, D.M., Chan, M.A., 2011. Stratigraphy and chronology of offshore to nearshore deposits associated with the Provo Shoreline, Pleistocene Lake Bonneville, Utah. Palaeogeography, Palaeoclimatology, and Palaeoecology 310, 442–450.

Goebel, T., 2007. Pre-Archaic and Early Archaic technological activities at Bonneville Estates Rockshelter: a first look at the lithic artifact record. In: Graf K., Schmitt, D. (Eds.), Paleoarchaic or Paleoindian? Great Basin Human Ecology at the Pleistocene-Holocene Transition. The University of Utah Press, Salt Lake City, Utah, pp. 156–184.

Goebel, T., and Keene, J.L., 2014. Are Great Basin Stemmed Points as old as Clovis in the intermountain west? A review of the geochronological evidence. In: Parezo, N.J., Janetski, J.C. (Eds.), Archaeology in the Great Basin and Southwest: Papers in Honor of Don D. Fowler. University of Utah Press, Salt Lake City, Utah, pp. 35–60.

Goebel, T., Hockett, B., Rhode, D., Graf, K., 2021. Prehistoric human response to climate change in the Bonneville basin, western North America: the Bonneville Estates Rockshelter radiocarbon chronology. Quaternary Science Reviews 260, 106930. https://doi.org/10.1016/j.quascirev.2021.106930.

Graf, K., 2007. Stratigraphy and chronology of the Pleistocene to Holocene transition at Bonneville Estates Rockshelter, eastern Great Basin. In: Graf, K., Schmitt, D. (Eds.), Paleoindian or Paleoarchaic? Great Basin Human Ecology at the Pleistocene-Holocene Transition. The University of Utah Press, Salt Lake City, Utah, pp. 82–104.

Graf K., Schmitt, D. (Eds.), 2007. Paleoarchaic or Paleoindian? Great Basin Human Ecology at the Pleistocene-Holocene Transition. The University of Utah Press, Salt Lake City, Utah.

Grayson, D.K., 2011. The Great Basin during the Holocene. In: Grayson, D.K. (Ed.), The Great Basin: A Natural Prehistory Revised and Expanded Edition. University of California Press, Berkeley, California, pp. 217–286.

Hall, S.A., Penner, W.L., Palacios-Fest, M.R., Metcalf, A.L., Smith, S.J., 2012. Cool, wet conditions late in the Younger Dryas in semi-arid New Mexico. Quaternary Research 77, 87–95.

Harris-Parks, E., 2016. The micromorphology of Younger Dryas-aged black mats from Nevada, Arizona, Texas and New Mexico. Quaternary Research 85, 94–106.

Hart, W.S., Quade, J., Madsen, D.B., Kaufman, D.S., Oviatt, C.G., 2004. The ^{87}Sr/^{86}Sr ratios of lacustrine carbonates and lake-level history of the Bonneville paleolake system. Geological Society of America Bulletin 116, 1107–1119.

Haynes, C.V., Jr., 1967, Quaternary geology of the Tule Springs Area, Clark County, Nevada. In: Wormington, H.M., Ellis, D. (Eds.), Pleistocene Studies in Southern Nevada. Nevada State Museum Anthropological Papers no. 13, Carson City, Nevada, pp. 15–104.

Haynes, C.V., Jr., 2008. Younger Dryas "black mats" and the Rancholabrean termination in North America. Proceedings of the National Academy of Sciences of the United States 105, 6520–6525.

Haynes, C.V., Jr., Huckell, B.B., 2007. Murray Springs: A Clovis Site with Multiple Activity Areas in the San Pedro Valley, Arizona. Anthropological Papers of the University of Arizona, No. 71. The University of Arizona Press, Tucson, Arizona.

Haynes, G.M., 2004. An Evaluation of the Chronological Relationships between Great Basin Stemmed and Pinto Series Projectile Points in the Mojave Desert. In: Allen, M.W., Reed, J. (Eds.), The Human Journey and Ancient Life in California's Deserts: Proceedings from the 2001 Millennium Conference. Maturango Museum, Ridgecrest, California, pp. 117–128.

Hirschi, J., 2006. Spatial Patterning of Late Paleoindian Stone Tools and Old River Paleochannels at Wild Isle, Utah [M.A. thesis]. Colorado State University, Fort Collins, Colorado.

Hockett, B., Goebel, T., 2019. The projectile points from Bonneville Estates Rockshelter: description of two new point types and implications for the long and short chronology debate in the Great Basin. Nevada Archaeologist 31, 9–50.

Horwitz, P.E., Chiarizia, R., Dietz, M.L., 1992. A novel strontium-selective extraction chromatographic resin. Solvent Extraction and Ion Exchange 10, 313–336.

Hoskins, A., 2016. Evaluating the Antiquity and Morphology of Corner-notched Dart Points in the Eastern Great Basin [M.A. Thesis]. Department of Anthropology, University of Nevada, Reno, Nevada. https://scholarworks.unr.edu/handle/11714/2167.

Janetski, J.C., Bodily, M.L., Newbold, B.A., Yoder, D.T., 2012. The Paleoarchaic to Early Archaic transition on the Colorado Plateau: the archaeology of North Creek Shelter. American Antiquity 77, 125–159.

Krzymińska, J., Namiotko, T., 2011. An overview of the Quaternary Ostracoda from the Gulf of Gdansk, the Baltic Sea. Joannea Geologie und Paläontologie 11, 104–106.

Lightfoot, K.G., Cuthrell, R.Q., Striplen, C.J., Hylkema, M.G., 2013. Rethinking the study of landscape management practices among hunter-gatherers in North America. American Antiquity 78, 285–301.

Lister, K.H., 1975. Quaternary freshwater Ostracoda from the Great Salt Lake Basin, Utah. The University of Kansas Paleontological Contributions, Paper 78, 1–40.

Madsen, D.B., 2016. The early occupation of the Bonneville Basin. In: Oviatt, C.G., Shroder, J.F., Jr. (Eds.), Lake Bonneville: A Scientific Update. Elsevier, New York, pp. 504–525.

Madsen, D.B., Oviatt, C.G., Young, D.C., Page, D.J., 2015a. Old River Bed Delta geomorphology and Chronology. In: Madsen, D.B., Schmitt, D.N., Page, D.J. (Eds.), The Paleoearchaic occupation of the Old River Bed Delta. University of Utah Anthropological Paper 28. Salt Lake City, The University of Utah Press, pp. 30–60.

Madsen, D.B., Schmitt, D.N., Page, D. (Eds.), 2015b. The Paleoearchaic occupation of the Old River Bed Delta. University of Utah Anthropological Paper 28. Salt Lake City, The University of Utah Press.

McCarthy, T.S., Ellery, W.N., 1998. The Okavango Delta. Transactions of the Royal Society of South Africa 52, 157–182.

Meisch, C., 2000. Freshwater Ostracoda of Western and Central Europe. Spektrum Akademischer Verlag GmbH, Heidelberg, Berlin, 522 p.

Meltzer, D.J., Holliday, V.T., 2010. Would North American Paleoindians have noticed Younger Dryas age climate changes? Journal of World Prehistory 23, 1–41.

Morrison, R.B., 1991. Quaternary stratigraphic, hydrologic, and climatic history of the Great Basin, with emphasis on Lake Lahontan, Bonneville, and Tecopa. In: Morrison, R.B. (Ed.), Quaternary Nonglacial Geology; Conterminous U.S. The Geology of North America. Geological Society of America, Boulder, Colorado K-2, 283–320.

Oviatt, C.G., 1988. Late Pleistocene and Holocene lacustrine fluctuations in the Sevier Lake basin, Utah, U.S.A. Journal of Paleolimnology 1, 9–21.

Oviatt, C.G., 2002. Bonneville Basin lacustrine history: the contributions of G.K. Gilbert and Ernst Antevs. In: Hershler, R., Madsen, D.B., Currey, D.R. (Eds.), Great Basin Aquatic Systems History, Smithsonian Contributions to the Earth Sciences, 33. Smithsonian Institution Press, Washington, DC, pp. 121–129.

Oviatt, C. G., 2014. The Gilbert Episode in the Great Salt Lake Basin, Utah. *Utah Geological Society Miscellaneous Publication* **14–3**, 1–20.

Oviatt, C.G., 2015. Chronology of Lake Bonneville, 30,000 to 10,000 yr B.P. *Quaternary Science Reviews* **110**, 166–171.

Oviatt, C.G., 2017. Ostracodes in Pleistocene Lake Bonneville, eastern Great Basin, North America. *Hydrobiologia* **786**, 125–135.

Oviatt, C.G., Shroder, J.F., Jr., 2016. *Lake Bonneville: A Scientific Update.* Elsevier, Cambridge, Massachusetts.

Oviatt, C.G., Sack, D., Currey, D.R., 1994. The Bonneville Basin, Quaternary, Western United States. In: Gierlowski, K.E., Kelts, K. (Eds.), *Global Geological Record of Lake Basins: World and Regional Geology.* Cambridge University Press, Cambridge, United Kingdom pp. 371–375.

Oviatt, C.G., Thompson, R.S., Kaufman, D.R., Bright, J., Forester, R.M., 1999. Interpretation of the Burmester core, Bonneville Basin, Utah. *Quaternary Research* **52**, 180–184.

Oviatt, C.G., Madsen, D.B., Schmitt, D.N., 2003. Late Pleistocene and early Holocene rivers and wetlands in western Utah. *Quaternary Research* **60**, 200–210.

Oviatt, C.G., Miller, D.M., McGeehin, J.M., Zachary, C., Mahan, S., 2005. The Younger Dryas Phase of Great Salt Lake, Utah, USA. *Palaeogeography, Palaeoclimatology, Palaeoecology* **219**, 263–284.

Oviatt, C.G., Madsen, D.B., Miller, D.M., Thompson, R.S., McGeehin, J.P., 2015. Early Holocene Great Salt Lake, USA. *Quaternary Research* **84**, 57–68.

Palacios-Fest, M.R., 2010. Late Holocene paleoenvironmental history of the upper West Amarillo Creek Valley at archaeological site 41PT185/C, Texas, USA. *Boletín de la Sociedad Geológica Mexicana* **62**, 399–436.

Pfaff, L.J., Schulmeister, M.K., Cronin, T.M., Smith, A.J., Aber, J.S., 2005. Late Quaternary ostracodes as indicators of salinity conditions and paleohydrology in a mid-continent wetland, Cheyenne Bottoms, Kansas. *Geological Society of America, Abstracts with Programs* **37** (7), 244.

Pigati, J.S., Rech, J.A., Quade, J., Bright, J., 2014. Desert wetlands in the geologic record. *Earth Science Reviews* **132**, 67–81.

Pigati, J.S., Springer, K.B., Honke, J.S., 2019. Desert wetlands record hydrologic variability within the Younger Dryas chronozone, Mojave Desert, USA. *Quaternary Research* **91**, 51–62.

Pilsbry, H.A., 1948. Land Mollusca of North America (north of Mexico). Volume II Part 2. *The Academy of Natural Sciences of Philadelphia Monographs*, **3**: i-xlvii, 521–1113. Philadelphia [19 March].

Quade, J., Forester, R.M., Pratt, W.L., Carter, C., 1998. Black mats, spring-fed streams, and late-glacial-age recharge in the southern Great Basin. *Quaternary Research* **49**, 129–148.

Rasmussen, S.O., Andersen, K.K., Svensson, A.M., Steffensen, J.P., Vinther, B.M., Calusen, H.B., Siggaard-Andersen, M.-L., *et al.*, 2006. A new Greenland ice core chronology for the last glacial termination. *Journal of Geophysical Research* **111**, D06102. https://doi.org/10.1029/2005JD006079.

Reimer, P., Austin, W.E.N., Bard, E., Bayliss, A., Blackwell, P.G., Bronk Ramsey, C., Butzin, M., *et al.*, 2020. The IntCal20 Northern Hemisphere radiocarbon age calibration curve (0–55 cal k BP). *Radiocarbon* **62**, 725–757. https://doi.org/10.1017/RDC.2020.41.

Rhode, D., 2016. Quaternary vegetation changes in the Bonneville Basin. In: Oviatt, C.G., Shroder, J.F., Jr., (Eds.), *Lake Bonneville: A Scientific Update. Developments in Earth Surface Processes 20.* Elsevier, Amsterdam, pp. 420–441.

Rhode, D., Louderback, L.A., 2015. Bonneville Basin environments during the Pleistocene-Holocene transition. In: Madsen, D.B., Schmitt, D.N., Page, D. (Eds.), *The Paleoarchaic Occupation of the Old River Bed Delta.* University of Utah Anthropological Papers 128, 22–29.

Rhode, D., Madsen, D.B., Jones, K.T., 2006. Antiquity of early Holocene small-seed consumption and processing at Danger Cave. *Antiquity* **80**, 328–339.

Rick, T.C., Wah, J.S., Erlandson, J.E., 2012. Re-evaluating the origins of late Pleistocene fire areas on Santa Rosa Island, California, USA. *Quaternary Research* **78**, 353–362.

Rosencrance, R.L., 2019. *Assessing the Chronological Variation within Western Stemmed Tradition Projectile Points* [M.A. thesis]. Department of Anthropology, University of Nevada, Reno, Nevada. https://scholarworks.unr.edu/handle/11714/5790.

Rutherford, J., 2000. *Ecology Illustrated Field Guides.* Wilfrid Laurier University, Waterloo, Ontario. [http://info.wlu.ca/~wwwbiol/bio305/Database, accessed May 28, 2007]

Schmitt, D.N., Lupo, K.D., 2018. On early-Holocene moisture and small-mammal histories in the Bonneville Basin, western United States. *The Holocene* **28**, 492–498.

Schmitt, D.N., Madsen, D.B., Oviatt, C.G. Quist, R., 2007. Late Pleistocene/early Holocene geomorphology and human occupation of the Old River Bed Delta, Western Utah. In: Graf, K., Schmitt, D. (Eds.), *Paleoindian or Paleoarchaic?: Great Basin Human Ecology at the Pleistocene-Holocene Transition.* The University of Utah Press, Salt Lake City, pp. 105–119.

Smith, G.M., Duke, D., Jenkins, D.L., Goebel, T., Davis, L.G., O'Grady, P., Stueber, D., Pratt, J.E., Smith, H.L., 2020. The Western Stemmed Tradition: problems and prospects in Paleoindian archaeology in the Intermountain West. *PaleoAmerica* **6**, 23–42. https://doi.org/10.1080/20555563.2019.1653153

Springer, K.B., Manker, C.R., Pigati, J.S., 2015. Dynamic response of desert wetlands to abrupt climate change. *Proceedings of the National Academy of Sciences of the United States of America* **112**, 14522–14526.

Steffensen, J.P., Andersen, K.K., Bigler, M., Clausen, H.B., Dahl-Jenzen, D., Fischer, H., Goto-Azuma, K., *et al.*, 2008. High-resolution Greenland ice core data show abrupt climate change happens in few years. *Science* **312**, 680–684.

Stuiver, M., Reimer, P.J., Reimer, R.W., 2021. CALIB 8.2 [WWW program] at http://calib.org. [accessed June 26, 2021]

Sutton, M.Q., Basgall, M.E., Gardner, J.K., Allen, M.W., 2007. Advances in understanding Mojave Desert prehistory. In: Jones, T.L., Klar, K.A. (Ed.), *California Prehistory: Colonization, Culture, and Complexity.* AltaMira Press, Lanham, Maryland, pp. 229–245.

Whatley, R., 1983. Some simple procedures for enhancing the use of Ostracoda in palaeoenvironmental analysis: *Norwegian Petroleum Directorate Bulletin* **2**, 129–146.

Wigand, P.E., Rhode, D., 2002. Great Basin vegetation history and aquatic systems: the last 15,000 years. In: Herschler, R., Madsen, D.B., Currey, D.R. (Eds.), *Great Basin Aquatic Systems History.* Smithsonian Institution Press, Washington, D.C., pp. 309–368.

Wilkinson, I.P., Bubikyan, S.A., Gulakyan, S.Z., 2005. The impact of late Holocene environmental change on lacustrine Ostracoda in Armenia. *Palaeogeography, Palaeoclimatology, Palaeoecology* **225**, 187–202.

Willig, J.A., Aikens, C.M., Fagan, J.L. (Eds.), 1988. *Early Human Occupation in Far Western North America: The Clovis-Archaic Interface.* Nevada State Museum Anthropological Papers No. 21, Nevada State Museum, Carson City, Nevada.

Wolbach, W.S., Ballard, J.P., Mayewski, P.A., Adedeji, V., Bunch, T.E., Firestone, R.B., French, T.A., *et al.*, 2018. Extraordinary biomass-burning episode and impact winter triggered by the Younger Dryas cosmic impact ~12,800 years ago. 1. Ice cores and glaciers. *The Journal of Geology* **126**, 165–184. https://doi.org/10.1086/695703.

Wood, R.D. 1967. *Charophytes of North America: A Guide to the Species of Charophyta of North America, Central America, and the West Indies.* Memorial Union University of Rhode Island, Kingston, Rhode Island, 72 pp.